Journal of
Engineering Sciences
Faculty of Engineering
Assiut University
JES
مجلة
العلوم الهندسية
كلية الهندسة
جامعة أسيوط
journal homepage: http://jesaun.journals.ekb.eg

# Shaping the Future of Vertical Bone Augmentation: A Detailed Review of Additive Manufacturing and 3D Biodegradable Scaffolds

Received 10 April 2025; Revised 12 September 2025; Accepted 13 September 2025

**Sleem. A. Farag** [1]
**Refaie Omar** [2]
**Salman S.A** [3]
**Ahmed Barhoum** [4]
**G.A. Abdalla** [5]
**Abdalla Abdal-hay** [6]

**Keywords**
Alveolar bone; Biomaterials; Biodegradable scaffolds; Titanium and its alloys; Vertical bone augmentation

**Abstract:** Achieving effective alveolar bone augmentation in the vertical dimension presents a significant challenge in periodontal tissue regeneration, particularly for optimizing dental implant procedures. Sufficient alveolar bone height is crucial for successful implant placement. To achieve this, several surgical approaches—such as autologous bone block grafting, distraction osteogenesis, and guided bone regeneration (GBR)—are commonly used, often in combination with natural or synthetic grafting materials. However, these conventional methods face limitations, including morbidity, dimensional instability, structural weaknesses, handling difficulties, and high failure rates. Recent advancements in additive manufacturing, present innovative solutions by enabling the creation of 3D porous scaffolds with essential properties for effective vertical bone augmentation, such as high porosity, interconnected pore structures, and superior handling capabilities. This review highlights the latest developments in GBR techniques and the application of additive manufacturing to produce biodegradable 3D scaffolds for vertical bone enhancement. It critically assesses the roles and limitations of biodegradable polymeric and metallic membranes in this field and introduces an overview of recent progress in vertical bone augmentation with these advanced scaffolds, reflecting the current state and future directions of research.

## 1. Introduction

In recent decades, dentistry has transformed with the rise of endosseous implants, addressing the increasing demand for tooth replacement [1]. A critical challenge in this field is the reduction of alveolar bone volume due to irreversible bone resorption from tooth loss, trauma, or surgical procedures [1-3]. Notably, significant volume loss can occur within the first three months [4], averaging a decrease of 1.5–2 mm in vertical height

[1] Sleem_abdelstar@aun.edu.eg Assistant Lecturer, Dept. of Mining and Metallurgical Eng., Faculty of Engineering, Assiut University, Assiut 71511, Egypt
[2] dr_refaie@au.edu.eg – Lecturer, Dept. of Mining and Metallurgical Eng., Faculty of Engineering, Assiut University
[3] sa.salman@azhatr.edu.eg - professor, Dept. of Mining and Petroleum Eng., Faculty of Engineering, Al-Azhar University, Cairo11835, Egypt
[4] ahmed.abdelrasoul@vub.ac.be – Associate professor, Dept. of Chemistry, Faculty of Science, Helwan University, Cairo, Egypt
[5] go_abdalla@aun.edu.eg – professor, Dept. of Mining and Metallurgical Eng., Faculty of Engineering, Assiut University
[6] abdalla.ali@uq.edu.au –Associate professor, Mechatronics Technology Program., Faculty of Industry and Energy Technology, New Cairo Technological University, Cairo 11835, Egypt

https://doi.org/10.21608/jesaun.2025.374253.1474
This is an open access article under the CC BY-NC-ND license (http://creativecommons.org/licenses/by-nc-nd/4.0/).

and 40%–50% in horizontal width from its original size [5]. Vertical bone augmentation is essential for maintaining natural bone height, as the success of dental implants relies on adequate alveolar bone volume. While various surgical techniques and biomaterials have been developed to tackle the complexities of bone resorption, including autologous block grafts [6, 7] and guided bone regeneration (GBR), these methods often present challenges such as morbidity, compromised stability, and high failure rates.

Additive manufacturing (AM) technologies have emerged as a promising solution for vertical bone augmentation. By enabling the fabrication of customized three-dimensional (3D) scaffolds, AM supports bone tissue growth [8-12] through techniques that utilize ceramics, polymers, and personalized metal mesh scaffolds. These 3D-printed scaffolds feature interconnected pore networks that enhance tissue integration, with optimal characteristics such as mechanical strength, hydrophilicity, and specific surface topography being crucial for cell adhesion and proliferation [13, 14]. Scaffolds used in alveolar bone regeneration must have several key characteristics. The human bone has a total porosity ranging from 30% to 90% [15]; therefore, scaffolds should have porosity around 70% for new tissue penetration and vascularization [19, 20]. Additionally, the mechanical strength of the scaffold is crucial for supporting target cells, adjacent tissues, and newly generated tissues until the completion of tissue creation [13, 21, 22]. Furthermore, the degradation rate of a scaffold must align with the rebuilding processes of the target tissue, with an acceptable degradation period of 5–6 months for dentoalveolar restoration [23, 24]. The review provides a comprehensive analysis of advancements in Guided Bone Regeneration (GBR) techniques and Additive Manufacturing (AM) technologies, focusing on the interaction between biomaterials and scaffold design. It emphasizes the complexity of alveolar bone regeneration, including cementum and periodontal ligament tissues, underscoring the need for multiphasic scaffolds that replicate the native tissues' structure, composition, and biochemical characteristics. A major focus is on the development of biodegradable 3D scaffolds for vertical bone augmentation, aligning with current trends in regenerative medicine to support natural integration. The article also discusses innovations in biodegradable polymeric and metallic membranes that enhance the success of vertical bone augmentation procedures. Ultimately, it highlights recent achievements in using these biodegradable scaffolds, offering insights into innovative solutions that will guide future advancements in dental implantation and regenerative techniques.

## 2. Vertical Bone Augmentation Techniques

Vertical bone augmentation is a critical aspect of oral surgical procedures aimed at preserving the original bone height, which is a challenge that requires the formation and maintenance of extraskeletal bone [7, 25]. Various methods are employed to enhance alveolar bone volume in the context of oral and dental surgery. Skeikh et al. [26] introduced a classification of bone augmentation techniques based on graft vascularization induction [27, 28]. This classification encompasses micro anastomosed free bone flaps, distraction osteogenesis, pedicled segmental osteotomies, bone morphogenetic induction grafts, and non-vascularized bone grafts, with the latter further divided into bone grafts and GBR [27, 28]. Vertical bone augmentation methods—such as autologous block grafts stabilized with screw fixation, distraction osteogenesis, and guided bone regeneration using particulate grafts with meshes or barrier membranes—are generally regarded as technique-sensitive and often yield unpredictable clinical outcomes [7]. Despite autogenous block bone grafting being considered the gold standard for vertical bone augmentation, these techniques have drawbacks, including the need for a second surgery, substantial morbidity and blood loss at the

donor site, high graft resorption rates, and limited bone supply [29, 30]. Although advances have been made in addressing issues related to space maintenance, graft fixation, and predictability of bone formation, challenges, particularly those concerning bone resorption, persist in dental surgery [29].

The introduction of cone-beam computed tomography (CBCT), computer-aided design/manufacturing (CAD/CAM), and three-dimensional (3D) printing technologies has enabled the clinical use of patient-specific implants (PSIs) with the necessary rigidity and biocompatibility [31]. Recent developments in 3D printing technology hold immense potential for advancing vertical bone augmentation [11, 32, 33]. Diverse 3D printing methods have been employed for manufacturing 3D scaffolds, membranes, and patient-specific metal meshes. This technique enables the production of porous biomaterials with an interconnected pore network in a layer-by-layer manner, allowing the fabrication of customized patient-specific constructs. Additionally, 3D printing has been utilized to create a wide range of scaffold geometries efficiently, with high dimensional accuracy, and personalized for individual patients [11]. Combining this technology with conventional imaging techniques, such as computed tomography (CT) scanning, facilitates the creation of scaffolds with geometric features identical to those of the host tissue [34]. The subsequent section delves into the most crucial techniques for alveolar bone augmentation.

### 2.1. Guided Bone Regeneration (GBR) Technique

GBR stands is a pivotal technique for vertical bone augmentation [35]. In GBR, particulate graft materials are isolated from the surrounding soft tissues using a resorbable or non-resorbable membrane, which enables bone growth [36]. Additionally, the barrier membrane serves to stabilize the graft material, restrict graft resorption, and act as an occlusive barrier against regeneration and infiltration of the surrounding soft tissues [37]. Initially designed for creating implant sites in atrophic jaws, GBR techniques have evolved to address various bone defects, particularly in the alveolar bone [38-40]. While some cases may not necessitate the use of barrier membranes, relying solely on graft material to fill the defect [41], it has been observed that bone resorption occurs when autografts are used without the aid of membranes [42, 43]. Thus, the employment of rigid and stable membranes is crucial for providing space maintenance, preventing soft tissue growth, and ensuring effective vertical bone growth [41]. However, the use of membranes alone in GBR often encounters challenges, such as membrane compression into the defective space by overlying soft tissues in many cases [44-47]. An ideal barrier membrane should fulfill multiple requirements, including ease of clinical handling, effective space maintenance, exclusion of epithelial and connective tissues from the defect site, biocompatibility, non-immunogenicity, non-toxicity, and the ability to integrate with surrounding tissues [48, 49]. Collagen, frequently employed as a biodegradable and resorbable barrier membrane, is a popular choice [50]. Synthetic degradable and resorbable membranes, such as polylactic acid (PLA), polyglycolic acid (PGA), and their copolymers, have also been used [51, 52]. Non-degradable membranes, while advantageous in maintaining shape throughout treatment, require a second surgery for removal after the healing period. Therefore, degradable membranes have been developed, offering benefits in terms of reduced patient morbidity, trauma, and overall procedural costs. The classification of bone augmentation techniques based on graft vascularization induction, which was discussed in the previous section, is summarized in Table 1.

Despite the bioactivity of collagen compared to synthetic membranes, concerns about collapse into the defect have been raised, limiting the available volume for regenerating bone [17, 53]. It has been suggested that stiff resorbable membranes demonstrate comparable bone formation levels to non-resorbable membranes [54, 55]. Furthermore, resorbable membranes exhibit improved soft tissue response and better tissue integration compared to their non-resorbable counterparts [55, 56]. In seeking alternatives to current GBR membranes, metallic materials, particularly those enhancing

human body metabolism such as iron (Fe), magnesium (Mg), and zinc (Zn), have emerged as promising candidates for bone defect applications [54, 55]. Efforts have been made to tailor their mechanical properties and corrosion behavior to meet the requirements of bioabsorbable bone defect applications.

**Table 1: The classification of bone augmentation techniques**

| Technique | Advantages | Disadvantages | Clinical Predictability | References |
|---|---|---|---|---|
| Micro-anastomosed free bone flaps. | Enhanced resistance to, potential for primary osteogenesis and hypertrophy, and versatility | Donor site morbidity, technically demanding and longer operative time | High for large defects and complex reconstructions | [26-28] |
| Distraction osteogenesis | Gradual bone formation, with no need for bone graft in some cases, can address large defects. | Requires specialized equipment, longer treatment duration, and potential for complications | Good, especially for vertical augmentation and larger defects | [26-28] |
| Pedicled segmental osteotomies | Preserved blood supply, good for moderate defects | Limited bone quantity, restricted to adjacent bone, may not be suitable for large defects. | Moderate to high, dependent on the size and location of the defect | [26-28] |
| Bone morphogenetic protein (BMP) induction grafts | Enhanced bone formation, used with various graft materials | Excessive cost, potential for ectopic bone formation, dosage-dependent complications; reliability may vary based on carrier and delivery | Variable depends on the specific BMP, carrier, and clinical setting | [26-28] |
| Non-vascularized bone grafts | A simpler technique can use autogenous or allogenic bone | Relies on creeping substitution, potential for resorption, limited to smaller defects (<5 cm) | Less predictable for larger defects, better for smaller contained defects | [26-28] |
| GBR (Guided Bone Regeneration) | Versatile, used for various defect types, predictable for small to moderate defects | Requires space maintenance, membrane exposure risk, and limited bone formation volume | High for small to moderate defects, especially in the alveolar ridge | [57, 58] |

### 2.2. Additive Manufacturing (AM) Techniques for Fabrication of 3D Scaffolds and Membranes

AM refers to ASTM-defined processes that build objects layer by layer from digital models [59]. Recently, it has been demonstrated that additive manufacturing technology holds significant promise for advancing research on vertical bone augmentation [60]. Utilizing additive manufacturing techniques allows the fabrication of porous biomaterials with an interconnected pore network in a layer-by-layer fashion, enabling the creation of customized patient-matched constructs [61]. The quality of scaffolds depends on the biomaterials used and the construction methods employed to achieve total harmony with the original tissues [60]. Scaffold properties for vertical bone augmentation depend on their composition, architecture, and surface features [62]. Scaffold porosity, pore size, interconnectivity, and mechanical integrity strongly influence osteogenic cell behavior [63, 64]. The optimal scaffold for alveolar bone augmentation must fulfill several

requirements, including biocompatibility, physical properties that mimic natural bone, total integrity with the bone, and avoidance of persistent immune responses [64, 65].

Human trabecular bone has a total porosity ranging between 30% and 90%, necessitating scaffolds with porosity within this range, suitable pore size, and good interconnectivity for integration with native tissue [15]. An overall porosity of 70% has been applied in preclinical and clinical studies for alveolar bone regeneration applications [15, 66]. A pore diameter between 150 and 500 μm facilitates vascularization and penetration of new tissues without compromising scaffold mechanical strength or cell infiltration into inner surface areas [19, 20, 67]. It has been reported that a porosity range of 60% to 90% is suitable for bone regeneration, with a pore size above 100 microns required for cell and tissue infiltration and vascularization [15]. Pore size affects bone regeneration, with larger pores favoring vertical augmentation and smaller pores enhancing regeneration in bony defects [68]. To ensure space maintenance, scaffolds must be mechanically robust and withstand masticatory loads of 50–200 N, varying with age and jaw site [68]. The roughness and connectivity of scaffold surfaces are crucial for promoting blood vessel sprouting within the scaffold, facilitating rapid osteogenesis and mineralization. An ideal surface roughness for scaffolds is considered to be "microrough" (Ra: 2–3 μm) to promote protein and biofactor adsorption and adhesion from the extracellular matrix [13, 22]. Scaffolds should possess high strength to support target cells, surrounding tissues, and newly formed tissue until full tissue formation is achieved [21]. For alveolar scaffolds, matching the compressive strength of cancellous bone in the human mandible is crucial, which ranges between 0.22 and 10.44 MPa, with a mean value of 3.9 ± 2.7 MPa [69]. Lastly, ideal scaffolds should be biodegradable and bioresorbable after bone healing, within 5-6 months, which is considered the appropriate degradation period [24].

Various additive manufacturing technologies have been employed for scaffold fabrication for vertical bone augmentation, including particle leaching, gas foaming, freeze-drying, phase separation, fiber meshes/fiber bonding, melt molding, and solution casting [70]. Scaffolds fabricated using these methods exhibit heterogeneities in pore size, porosity, interconnectivity, and architecture.

SFF (or RP) techniques allow scaffolds to be fabricated with precise geometry and reproducible 3D architecture [71]. These technologies, often referred to as "3D printing" include inkjet printing, laser-assisted printing, and extrusion printing. Selective Laser Sintering (SLS) and stereolithography (SLA) are laser-assisted methods, whereas Fused Deposition Modeling (FDM) is a method developed for extrusion printing [72]. Each printing method is compatible with specific biomaterials, with laser-assisted methods suitable for a wide range of viscosities, inkjet printing for low-viscosity biomaterials, and extrusion printing restricted to thermoplastic biomaterials, such as PCL [73]. These techniques are particularly suitable for fabricating hydrogel scaffolds comprising natural and synthetic polymers [74]. Hydrogels and both natural and synthetic polymers have been widely explored for fabricating 3D scaffolds and membranes in bone tissue engineering because of their biocompatibility and versatile properties [75, 76]. However, their applications are limited by challenges such as mechanical weakness, swelling, and degradation [77, 78]. Although hydrogels offer excellent biocompatibility and a cell-friendly environment, their mechanical properties are often inadequate for load-bearing applications [78]. Natural hydrogels, such as collagen and alginate, tend to be mechanically weak [77]. Furthermore, hydrogels are characterized by their high-water content, which contributes to their biocompatibility but also leads to significant swelling in aqueous environments [79]. Uncontrolled swelling can cause structural instability and affect the mechanical integrity of scaffolds [80]. The swelling properties of hydrogels can be tuned by controlling their crosslinking density and polymer composition [79]. The degradation rate of hydrogels is a critical factor in tissue engineering, as it should ideally match the rate of new bone formation [75]. Natural polymers such as collagen, chitosan, and gelatin are favored for their

inherent bioactivity and similarity to the extracellular matrix (ECM) [81]. However, they often lack the mechanical strength required for structural support in tissue engineering applications [77]. For example, although collagen scaffolds can mimic trabecular bones, technological constraints limit the 3D printing of complex structures [82]. Synthetic polymers, including polycaprolactone (PCL) and poly (lactic acid) (PLA), offer better mechanical properties and controlled degradation rates than natural polymers [83]. However, they often lack cell-interactive signals present in natural materials, which can hinder cell adhesion and proliferation [77]. For instance, PCL has good biocompatibility and a slow degradation rate but may require modification to enhance cellular interaction [84]. Natural polymers exhibit swelling behavior that can be influenced by pH and ionic strength [80]. Excessive swelling can lead to scaffold degradation and loss of mechanical properties [80]. Synthetic polymers generally exhibit lower swelling than natural polymers and hydrogels. However, the hydrophobicity of certain synthetic polymers can limit cell infiltration and nutrient transport [83]. Natural polymers are generally biodegradable, but controlling their degradation rate can be challenging [81]. Synthetic polymers offer better control over degradation rates through careful selection of monomers and polymer architecture [85]. For instance, PCL degrades slowly, providing long-term mechanical support, whereas PLA degrades more rapidly [84]. Newer techniques leverage CAD and CAM technologies to 3D-print desired structures based on CAD files, thereby defining the exact dimensions of the fabricated scaffold [86].

### 2.2.1. Stereo lithography (SLA)

SLA is a 3D printing technique that has gained prominence in vertical bone augmentation. In this method, a liquid photopolymer resin is cured layer by layer using a laser beam, resulting in the formation of a solid 3D structure [87]. SLA offers several advantages over conventional manufacturing methods, particularly its capacity to craft intricate geometries and personalized implants tailored precisely to the patient's bone structure [74, 88]. An outstanding feature of SLA in vertical bone augmentation is the ability to fabricate customized scaffolds that align precisely with the unique specifications of a patient's bone structure. This is especially crucial in scenarios involving distinctive bone defects or complex implant geometries. Implants produced through SLA exhibit higher precision and accuracy than those produced using traditional manufacturing methods [74]. The potential of creating scaffolds using SLA holds promise for enhancing the success rate of bone augmentation procedures while concurrently reducing patient recovery time [74, 88].

SLA excels at generating scaffold geometries that may be challenging or unattainable using traditional manufacturing methods. This is invaluable when dealing with patients with complex bone defects or requiring implants with intricate geometries. Implants produced via SLA demonstrate a higher level of complexity than those manufactured using traditional methods. The capacity to create intricate implant geometries with SLA holds the potential to significantly improve the accuracy and efficacy of bone augmentation procedures. Beyond its geometric advantages, SLA has the potential to reduce costs and enhance the efficiency of bone augmentation procedures. Implants produced through SLA exhibit lower manufacturing costs than those produced using traditional methods. Moreover, SLA can reduce the time required for the production of customized implants, leading to cost savings and increased procedural efficiency [74, 89].

Despite these advantages, SLA has certain limitations in vertical bone augmentation. One limitation is the constrained mechanical properties of some SLA-produced materials, which exhibit lower mechanical strength compared to traditional manufacturing methods. Addressing this limitation may be possible in the future through advancements in material science and the development of new SLA-produced materials with improved mechanical properties [89]. Another limitation is the restricted size range of implants produced through SLA, which presents a challenge compared to traditional manufacturing methods.

Overcoming this limitation may be achievable through future advancements in SLA technology and the introduction of novel techniques for producing larger scaffolds [89, 90].

### 2.2.2. Selective Laser Sintering (SLS)

In SLS, a small bed of powdered material is heated just below its melting point and then fused using a potent carbon dioxide laser, binding the particles together [91]. Common materials employed in this procedure include polymer PCL, calcium phosphates, or composites of polymer, metal, thermoplastic, and bioceramic, which are applied as a fresh layer of powdered material for each iteration until the 3D scaffold is fully constructed [92]. It is important to note that natural polymers cannot be utilized in SLS because of the high temperatures generated by the laser. While SLS methods excel in producing highly detailed printed scaffolds with thin walls [92], they have drawbacks, such as poor dimensional accuracy within the range of 150–180 µm [93]. Furthermore, incorporating growth factors and cells during printing poses a challenge for SLS methods [93, 94]. The process is also susceptible to issues such as scaffold shrinking and warping due to thermal distortion [95]. Various scaffold materials fabricated using the L-PBF machine are shown in Figure 1. WE43 is an alloy composed of magnesium, yttrium, and rare-earth elements and is known for its excellent biocompatibility and mechanical properties. The biodegradability of the WE43 scaffold is a key advantage, as it gradually degrades over time, eliminating the need for surgical removal and reducing the risk of complications. This property also facilitates the integration of scaffolds with the surrounding tissue, promoting cell infiltration, neovascularization, and tissue regeneration. The use of biodegradable metal scaffolds made of L-PBF from WE43 holds great potential for vertical bone augmentation [96, 97]. A diamond lattice was adopted to construct a cylindrical porous scaffold, the design of which was the same as that of iron scaffolds prepared as shown in Figure 1(d-f) [98, 99]. The zinc scaffold, shown in Figure 1 (g-i), possesses biocompatibility, controlled degradation, and customizable pore size, enabling optimal tissue integration and regeneration. Their properties make them promising for enhancing bone formation in vertical bone augmentation procedures [99].

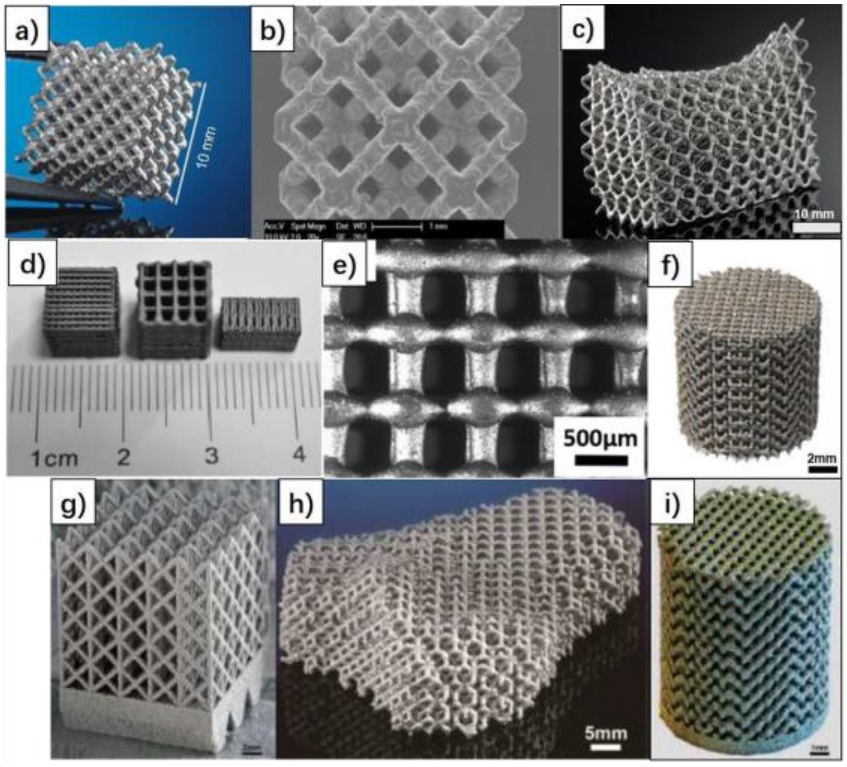


**Fig. 1: Biodegradable metal scaffolds made by L-PBF: (a-c) WE43 [96, 97], (d-f) pure Fe [98, 99], (g-i) pure Zn [100].**

### 2.2.3. Powder bed and inkjet head 3D printing (3DP)

In additive manufacturing (AM), powder bed and inkjet head 3D printing (3DP) systems are notable for their versatility. An inkjet head deposits a liquid-fusing substance onto a powder bed, binding particles together [101]. There are variations, including thermal printing, which uses localized temperatures (100-300 °C) to create bubbles for droplet ejection, and piezoelectric printing, which generates droplets using pressure or acoustic waves [102]. While thermal inkjet printing faces challenges with shear and thermal stresses [103], especially for natural polymer inks [104], piezo inkjet printing is cost-effective and adaptable to various materials, though it requires low-concentration inks [105]. This technique is particularly beneficial for creating bone scaffolds due to its flexible material options, as long as the materials are in powder form [106]. Figure 2 illustrates the two different mechanisms employed in powder bed inkjet printing, highlighting its potential for creating a wide range of materials into intricate and customized bone scaffolds [106].

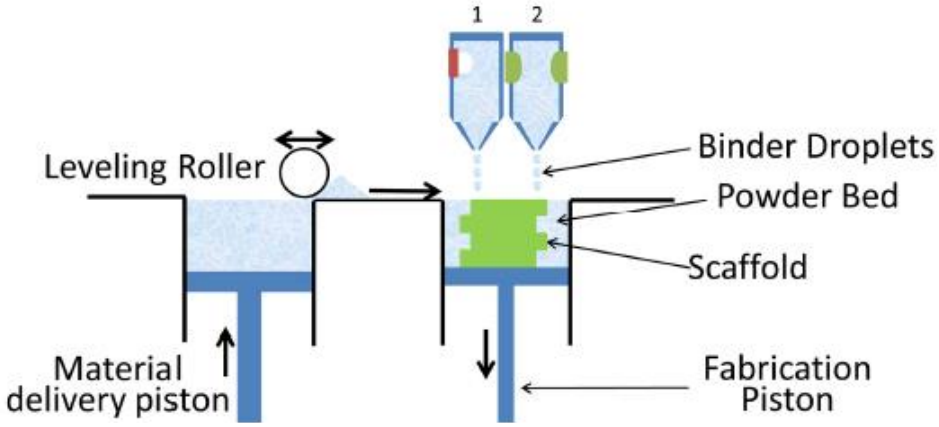


**Fig. 2: Two inkjet printing mechanisms, thermal-based and piezoelectric-based, operating on a powder bed. Inkjet printheads apply a binding solution to the powder. Reproduced with permission from [106].**

### 2.2.4. Extrusion Printing (Fused deposition modeling (FDM))

Extrusion printing, commonly known as FDM, has emerged as a noteworthy contender in the realm of vertical bone augmentation. This technique shows promise for crafting personalized scaffolds with intricate geometries tailored to individuals with varying degrees of bone loss. Extrusion printing encompasses methods like fused deposition modeling (FDM) and the extrusion of gelling liquid materials. In the fused deposition modeling (FDM) method, the material is heated until it reaches a molten state, subsequently being extruded through a nozzle via pressured extrusion, screw-based extrusion, or a hybrid of both [107]. The precision and form of the final scaffold hinge on the rate at which the molten extruded filament cools and solidifies post-dispensation. However, this method is confined to the fabrication of biodegradable materials such as PCL and PLA, along with metal 3D scaffolds [107]. Extrusion printing techniques boast advantages such as cost-effectiveness and rapid processing speed [108]. Nonetheless, challenges like low resolution (approximately 200 µm) [109] and the necessity for high-viscosity inks are acknowledged as drawbacks associated with these methods. Despite these limitations, the versatility and suitability of extrusion printing make it a noteworthy player in the landscape of additive manufacturing for vertical bone augmentation.

One of the main challenges with FDM products is surface roughness [110]. This can be addressed through pre-manufacturing methods, such as optimizing design parameters like layer thickness and part orientation, or through post-processing techniques [111]. Heshmat et al. carried out a number of investigations to look at how various FDM processes affected the products' rough surface. In order to improve surface roughness, they look at an online polishing method that uses a hot-air jet applied concurrently during the printing process [112]. It has been demonstrated that the hot-air jet

improves average roughness by 65.3% by locally melting the staircase effect on the surface, making it smoother [112]. In a similar study, Heshmat et al. investigated the effectiveness of slurry impacts in improving the roughness of the surface parts made using FDM. They utilized a silica-water mixture to soften the surface's staircase effect during the process. The results showed that the surface roughness has significantly decreased by more than 70% in the traverse direction and more than 40% in the longitudinal direction [113].

In another study, Heshmat et al. explores the enhancement of surface roughness in 3D printed PLA by examining three factors: printing orientation, layer thickness, and slurry impact angle. A Whirling Arm Slurry Test (WASET) rig is used to assess these effects. The results indicated a 42% improvement in surface roughness in the transverse direction and a 24% improvement in the longitudinal direction. Also, they developed an Adaptive Neuro-Fuzzy Inference System (ANFIS) model to effectively predict surface roughness values. Optimal conditions for minimizing surface roughness were identified as a medium layer thickness of 0.2 mm, a building orientation of 40°, and an impact angle of 45°. The model demonstrated precise output values, confirming its effectiveness [114].

### 2.2.5. CAD/ CAM methods

In recent developments, cutting-edge techniques leverage Computer-Aided Design (CAD) and Computer-Aided Manufacturing (CAM) technologies to facilitate the 3D printing of structures based on predefined CAD files, specifying precise scaffold dimensions [115]. This innovative approach has revolutionized the landscape of bone reconstructive surgery planning, considering aesthetic, prosthetic, and functional requirements [115]. The integration of CAD-CAM technologies introduces novel solutions for surgical planning, particularly in bone reconstructive procedures. By utilizing images from computed tomography (CT) scans, CAD models are meticulously crafted to address patient-specific bone defects, leading to the creation of a bespoke bone graft substitute [116, 117].

### 2.2.6. Other methods

Continuous Filament Fabrication (CFF) stands as a fabrication method akin to Fused Deposition Modeling (FDM), employing a polymeric filament locally molten in the printing head. The extrusion force is generated through filament movement facilitated by rollers, offering a unique approach to 3D scaffold manufacturing [118]. Primarily used for nylon and Kevlar, CFF contributes to the production of robust and tailored 3D scaffolds. Another noteworthy method is Direct Ink Writing (DIW), an innovative approach to scaffold fabrication involving the extrusion of polymeric ink or a binder. This process yields scaffolds with high resolution, although the initially produced objects tend to be soft and fragile. Concurrent printing of support materials is common to address this limitation. Post-printing steps, including drying, debinding, and sintering, are crucial for optimizing mechanical characteristics [119]. DIW demonstrates compatibility with a diverse range of materials, including ceramics, ceramic and metal matrix composites, sol-gel, and polymers [120]. **Table 2** offers a comprehensive overview of the concepts and applications of 3D-printed scaffolds in the realm of bone tissue engineering, showcasing the diverse capabilities and potential applications of these advanced fabrication techniques.

Furthermore, the different types of scaffold materials and their additive manufacturing approaches, emphasizing their biodegradability, mechanical strength, bioactivity, and clinical applicability, are summarized in **Table 3**.

**Table 2: Principles and applications of 3D printing of vertical augmentation scaffolds**

| Class | Manufacturing method | Advantage | Disadvantage | Reference |
|---|---|---|---|---|
| Extrusion | Fused deposition modeling (FDM | Low cost, simple manufacturing, creating layer bonding, and a wide application range. | Low precision, only thermoplastic materials, rough surface, and slow speed. | [121, 122] |
| | Direct ink writing/ robocasting (DIW) | Fast printing speed, easy operation, low cost and high precision | Low molding accuracy and easy to deform. | [123] |
| | Stereolithography (SLA) | Fast processing speed, high maturity, Namoura materials options, and high precision. | High cost, software operation difficulty, and high environmental requirements. | [124, 125] |
| Powder bed | Powder bed and inkjet head 3D printing (3DP) | Printable active substances and prepared complex scaffolds. | Long drying time and ink are prone to deteriorating. | [126] |
| | Electron beam additive manufacturing (EBM) | Wide selection of Materials without adding organic adhesives. | High cost and low efficiency. | [127] |
| | Selective laser sintering (SLS) | | | |

**Table 3: Summarizing scaffold material types via their characteristics**

| Scaffold Type | Material | Additive Manufacturing Approach | degradability | Mechanical Strength | Bioactivity | Clinical Applicability | Ref. |
|---|---|---|---|---|---|---|---|
| **Natural Polymers** | Collagen, Chitosan, Alginate, Fibrin, Hyaluronic Acid | FDM, SLS | High | Moderate | High | Widely used | [128] |
| **Synthetic Polymers** | PLA, PGA, PCL, PLGA | FDM, SLS | High | Moderate | Moderate | Widely used | [128-131] |
| **Ceramic** | Hydroxyapatite, TCP | SLS,3D Printing | Moderate | High | High | Limited | [132, 133] |
| **Metal Scaffolds** | Titanium, Magnesium, zinc | AM, SLM | Low | Very High | Low | Emerging | [133, 134] |
| **Composite Scaffolds** | Polymer-Ceramic Hybrid | FDM, SLS | Variable | High | High | Emerging | [131, 135] |

## 3. Degradable bio-membrane for vertical bone augmentation

Barrier membranes are frequently used in dental surgery to encourage GBR. To allow new bones to fill the space left by bony defects and restore functioning, the barrier membrane is positioned to prevent the gingival soft tissues from migrating into the area. Both biodegradable resorbable and biodegradable non-resorbable membranes are used in GBR. There are two prominent types of bio-degradable membranes are polymeric membranes and metallic membranes, each offering unique advantages and challenges. Polymeric membranes, typically made from materials like polycaprolactone (PCL) or polylactic acid (PLA), are favored for their biocompatibility and controlled degradation rates. These membranes provide a flexible, lightweight option that can conform to various anatomical shapes, promoting effective bone regeneration. Their gradual degradation allows for sustained support during the healing process while minimizing the risk of inflammatory responses. Conversely, degradable metallic membranes provide superior mechanical strength and stability. Their robust structure makes them ideal for applications requiring significant load-bearing capacity. However, the long-term presence of metals can induce foreign body reactions, potentially complicating healing. The distinct properties and applications of both polymeric and metallic membranes in vertical bone augmentation are summarized in Table 4, highlighting their respective benefits and limitations.

**Table 4: Properties of bio-degradable polymeric and metallic membranes.**

| Feature | Degradable Polymeric Membranes | Degradable Metallic Membranes | References |
|---|---|---|---|
| Mechanical Strength | Lower mechanical strength compared to metallic membranes. | High mechanical strength. | [136-138] |
| Space Maintenance | Maintaining space for bone regeneration can be challenging, especially in large vertical defects, often used with bone grafts or bone substitutes to provide initial support. | Excellent space maintenance due to inherent rigidity, and it can be shaped to fit the defect precisely. | [139, 140] |
| Preferable scenarios | Small to moderate vertical defects. Sites with good soft tissue coverage | Large vertical defects Sites with compromised soft tissue coverage. | [137, 139] |
| Complications | Potential for premature degradation, compromising space maintenance; inflammatory reactions to degradation products may occur. Risk of membrane collapse if not properly supported. | Risk of soft tissue dehiscence and membrane exposure.<br>Potential for infection. | [140, 141] |

### 3.1. Degradable Polymeric Membrane for Vertical Bone Augmentation

GBR emerges as a pivotal technique in vertical bone augmentation, particularly in maxillary and mandibular alveolar bones. This method uses a barrier membrane to control blood clots, secure space for newly formed bone, and exclude soft tissue [36, 142].

#### 3.1.1. A biodegradable polymeric membrane compared with the titanium membrane

A notable innovation in this domain involves the use of 3D membranes composed of a slow-degrading polymer (polycaprolactone, PCL) and a rapidly degrading polymer (poly-lactic-co-glycolic acid, PLGA 85/15) as introduced by Kim et al [143-145]. Kim et al. [143] employed MHDS to produce 3D membranes from a PCL/PLGA/β-TCP composite [143], whose half-life in vivo was around 9 weeks previously reported for a porous sponge [146]. Furthermore, the

combination of 3D polymeric membranes with particulate materials, such as bone morphogenetic proteins (BMPs), has been explored for enhancing vertical bone augmentation.

Shim et al. carried out multiple studies examining the efficacy of rhBMP-2-loaded PCL/PLGA/β-TCP GBR membranes [143, 144, 147]. These 3D-printed membranes, characterized by their small pore sizes, demonstrated significant results in promoting bone formation and enhancing osseointegration. In a rabbit model, the researchers evaluated the performance of the rhBMP-2-loaded membranes in reconstructing calvarial defects. The findings revealed that the BMP-2-loaded membranes significantly outperformed the control group, effectively facilitating bone formation and filling interstitial spaces by 8 weeks post-implantation [143].

Comparatively, a study by Shim et al. [144] compared the effects of a 3D-printed (PCL/PLGA/β-TCP) membrane with a titanium mesh membrane using extrusion-based 3D printing technology. The study, conducted on beagle dogs, revealed significant new bone formation around implants in buccal defect regions for the PCL/PLGA/β-TCP group. Notably, the membrane was either fully or partially absorbed, or retained bone graft materials were surrounded by bony tissues. In contrast, the control group exhibited minimal bone formation, emphasizing the efficacy of the 3D-printed membrane in osseointegration as illustrated in Figure 3. However, challenges arise with the rapid degradation of PLGA, potentially triggering inflammatory reactions and compromising mechanical properties in the longer term. These findings underscore the potential of 3D-printed polymeric membranes, emphasizing their role in advancing GBR techniques for vertical bone augmentation.

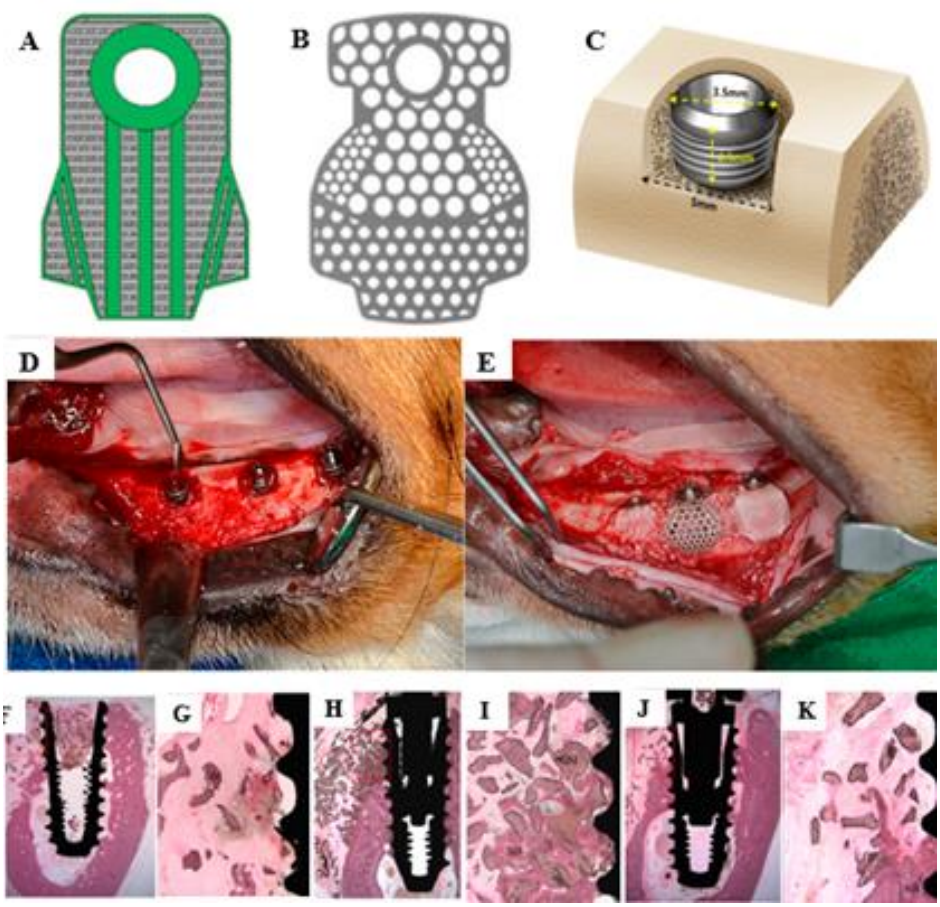


**Fig. 3: Efficacy of 3D-printed composite GBR membranes 8 weeks post-implantation. (A): 3D CAD model design of the PCL/PLGA/β-TCP membrane; (B), Titanium mesh design. (C) The open buccal defect model. (D, E): Surgical protocol shows the placement of a dental implant overlayed by the 3D-printed membrane. (F-K): tissue morphology of the various groups (F, G): no membrane, (H, I) 3D-printed membrane, (J, K): Titanium membrane [144].**

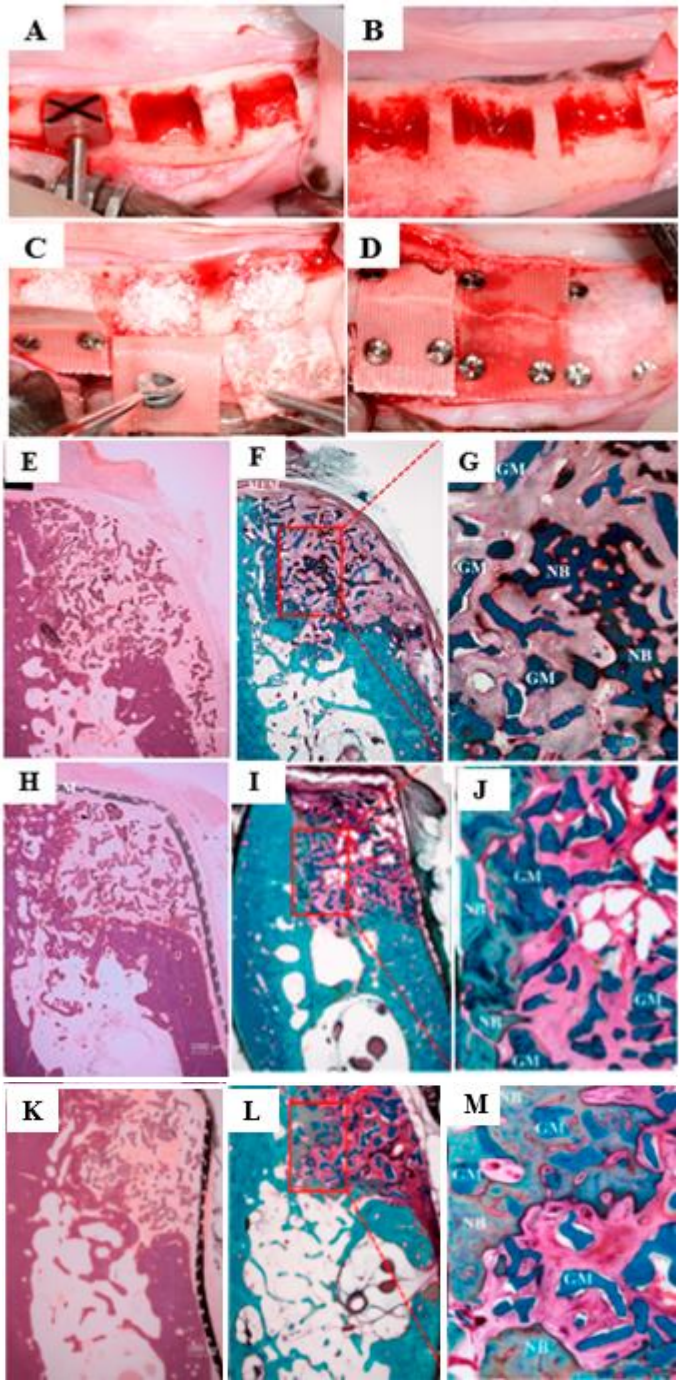


**Fig. 4: Comparison of PCL and PCL/β-TCP 3D-printed membranes with a collagen membrane in a canine mandibular defect model. (A, B) Surgical preparation of standardized defects. (C) Implantation of particulate bone graft materials. (D) Placement of membranes (collagen, PCL, or PCL/β-TCP) fixed with titanium screws. (E–M) Histological evaluation: Hematoxylin and eosin staining (E, H, K) and Goldner's Trichrome staining (F, G, I, J, L, M) for collagen (E–G), PCL (H–J), and PCL/β-TCP membranes (K–M) [147].**

### 3.1.2. Biodegradable polymeric membrane compared with collagen membrane

Building on their earlier research, Shim et al. [147] evaluated the effectiveness of 3D-printed PCL and PCL/β-TCP membranes (in a 4:1 weight ratio) compared to a conventional commercial collagen membrane for facilitating guided bone regeneration (GBR) in a canine model, as illustrated in Figure 4 A-D. A 175 $mm^3$ defect was created across six mandibular sites in three different animals. The membranes were secured with titanium pins, with bovine graft particulate placed

beneath each, and healing was monitored for over 8 weeks. The results indicated no significant differences in the amount of bone formed between the collagen and 3D-printed membranes, as shown in Figure 4 E-M.

Despite variations in pore sizes, the PCL 3D-printed membrane demonstrated superior long-term space maintenance and handling capabilities compared to the hydrated collagen membrane, which tends to lose stiffness and handling ability upon exposure to biological fluids. The use of a polymer/ceramic composite scaffold for bone augmentation yielded promising results; however, reliance on bone grafting materials raises concerns regarding handling and stability. Furthermore, inadequate stress distribution across the membrane may hinder effective bone regeneration, and insufficient control over the volume of regenerated bone could impede the jawbone's ability to restore its original anatomical structure.

### 3.2. Degradable bio-metallic membrane for Vertical Bone Augmentation

In the field of maxillofacial surgery, GBR employing membranes or meshes is a common practice to augment alveolar bone volume and stimulate bone regeneration within bony windows or defects [148, 149]. Various biomaterials, including non-resorbable metals such as titanium [150] and stainless steel [151], have been utilized as membranes in GBR due to their exceptional mechanical properties, preventing bony defects from collapsing and facilitating new bone formation. However, the differing elastic modulus compared to natural bone poses challenges such as stress-shielding effects, mastication-related issues, and the potential for long-term inflammatory responses and mesh exposure, necessitating surgical removal of the bio-inert membrane and causing tissue damage and discomfort [152]. To overcome the limitations associated with non-degradable membranes, there has been recent interest in the development of biodegradable metallic membranes for GBR. Magnesium and its alloys, in particular, have emerged as promising materials due to their sufficient rigidity for maintaining space at the site and supporting long-term new bone formation, in contrast to conventional bioresorbable polymeric membranes [153].

Rider et al [154] investigated a biodegradable magnesium membrane (30 × 40 mm with a thickness of 140 μm) created using a hot-rolling technique from high-purity magnesium sheets (99.95%) in a Beagle dog model, as shown in Figure 5A-F. The preparatory phase involved the extraction of four teeth, specifically from the mandibular second premolar to the first molar (PM2 to M1) on both sides of the lower mandible, along with corresponding upper maxillary teeth. Following this, the upper jaw was closed, allowing for a healing period of 12 ± 2 weeks, with sutures removed approximately 2 ± 1 weeks post-extraction (Figure 5G-H).

In the experimental phase, two 5 mm diameter and 5 mm deep bone defects were created on each side of the lower jaw. These defects were filled with BioOss (Geistlich AG) and covered with either the magnesium membrane or a collagen membrane (Bio-Gide, Geistlich AG), secured in place using four titanium screws. The study included mechanical tests to evaluate the properties of the magnesium membrane, as well as an in vitro corrosion assessment.

Results showed that during the initial 8-week healing period, the magnesium membrane effectively maintained its barrier function, providing space while securely holding the bone graft material within the defect space, facilitating bone regeneration. In the subsequent phase, a salty corrosion layer and local gas cavities formed, sustaining the separation between soft and hard tissues. At week 16 post-implantation, the magnesium membrane was fully corroded and resorbed. The in vivo performance study demonstrated its comparable healing response and tissue regeneration to a resorbable collagen membrane, suggesting its suitability as a barrier membrane in GBR treatment. A static tensile strength test revealed a maximum tensile stress of 183.0 ± 10.7 MPa [155]. The magnesium membrane exhibited high resistance to collapse, potentially preventing the reported risk

observed with collagen [156, 157] and polymeric membranes. Moreover, Mg displayed an increase in resistance to puncture even after 7 days of degradative conditions compared to the undegraded collagen membrane. The fixation of the magnesium membrane using a titanium fixation screw could form a galvanic cell between magnesium and titanium. This galvanic cell leads to an increase in the dissolution rate of magnesium and the hydrogen evolution on the titanium screw surface. They assessed the effect of the galvanic corrosion cell between the magnesium membrane and titanium screw using voltammetry measurements in Hank's Balanced Salt Solution (HBSS) with varying surface area ratios between the magnesium membrane and titanium. The result revealed that the surface area ratio of 10 (Mg):1(Ti) or higher does not enhance the risk of local galvanic corrosion. In addition, a homogenous corrosive attack was confirmed by microscopic observations of the magnesium membranes, which were fixed by titanium screws in HBSS up to 54 h. An interesting finding in this study is the effect of hydrogen gas that is released due to the degradation process of the magnesium membrane. The released hydrogen gas creates an additional barrier between the soft and the hard tissues due to the formation of a thin gas pocket layer on the upper surface of the membrane towards the soft tissue. Therefore, the hydrogen gas that is formed above the membrane does not affect bone regeneration, and these results agree with the reported results from [154, 158].

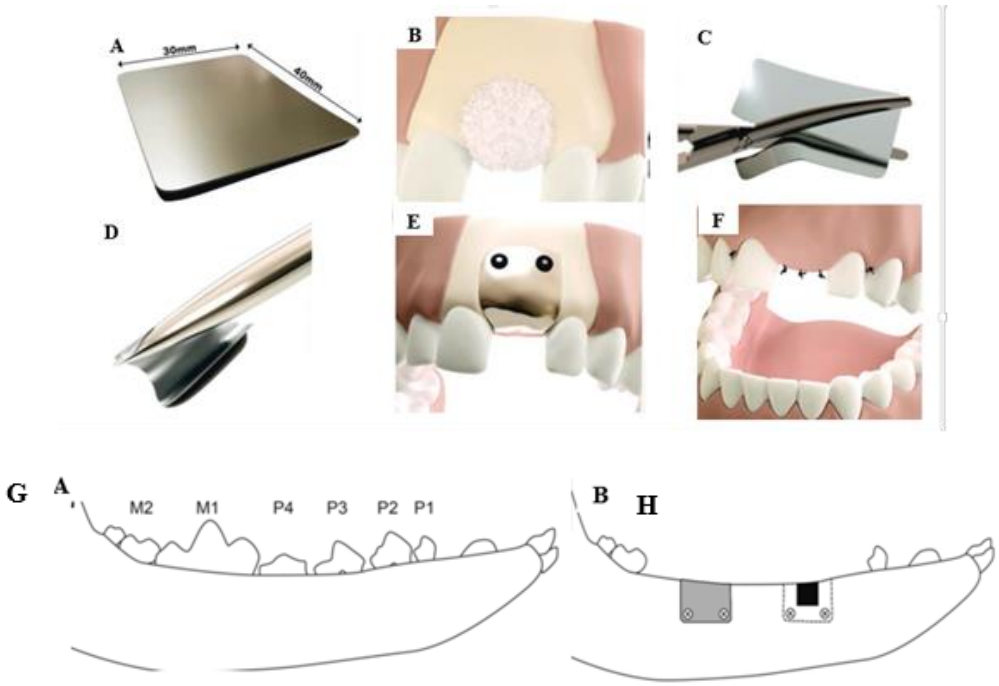


**Fig. 5: Surgical procedure using a magnesium (Mg) membrane. (A) Shape of the Mg membrane. (B) Defect site without Mg membrane. (C) Cutting the Mg membrane. (D) Covering the defect with the Mg membrane. (E) Fixation of the Mg membrane on both buccal and palatal/lingual sides. (F) Reflection of the mucoperiosteal flap. (G) Anatomical site: four teeth between the mandibular second premolar (PM2) and first molar (M1). (H) After a healing period of 12 ± 2 weeks, two independent bone defects were created on each side of the mandible [154].**

Yan et al. [159] investigated the viability and effectiveness of a degradable magnesium alloy, specifically (Mg-2Zn-0.46Y-0.5Nd), for repairing distal bone defects (DBD) in the mandibular second molar (M2M) using a novel M2M-DBD model with beagle dog mandibles. The study involved eight beagle dogs, where a standardized two-wall bony defect (5 mm × 5 mm × 5 mm) was surgically created by removing the distal roots to simulate M2M-DBD conditions, as shown in Figure 6 (a-i). The thirty-two bone defects were randomly divided into four groups based on the

GBR membrane used, with two groups utilizing the MAR-Gide (MG) membrane and the others employing the Bio-Gide (BG) membrane. Histological analysis presented in Figure 6 (j-o) revealed complete degradation of the MG membrane within three months post-surgery. The MG membrane demonstrated favorable in vivo biocompatibility, not associated with subcutaneous emphysema or an increased risk of infection compared to the BG membrane. Additionally, MG exhibited potential osteoinductive properties, with its osteogenic effects comparable to those of BG, showing no significant differences in vertical bone height or the percentage of new bone formation (45.44 ± 12.28% for MG vs. 43.49 ± 7.12% for BG). Importantly, the MG-6m group histologically showed no gas cavity, as depicted in Figure 6 (n, o). The degradation products of magnesium were closely linked to new bone, indicating that they did not impede bone formation. While enhancements to the Mg alloy could improve the osteogenic effects of the MG membrane, the study highlighted a key limitation, underscoring the necessity for future research to establish the optimal degradation rate that supports adaptation to bone formation in the oral cavity.

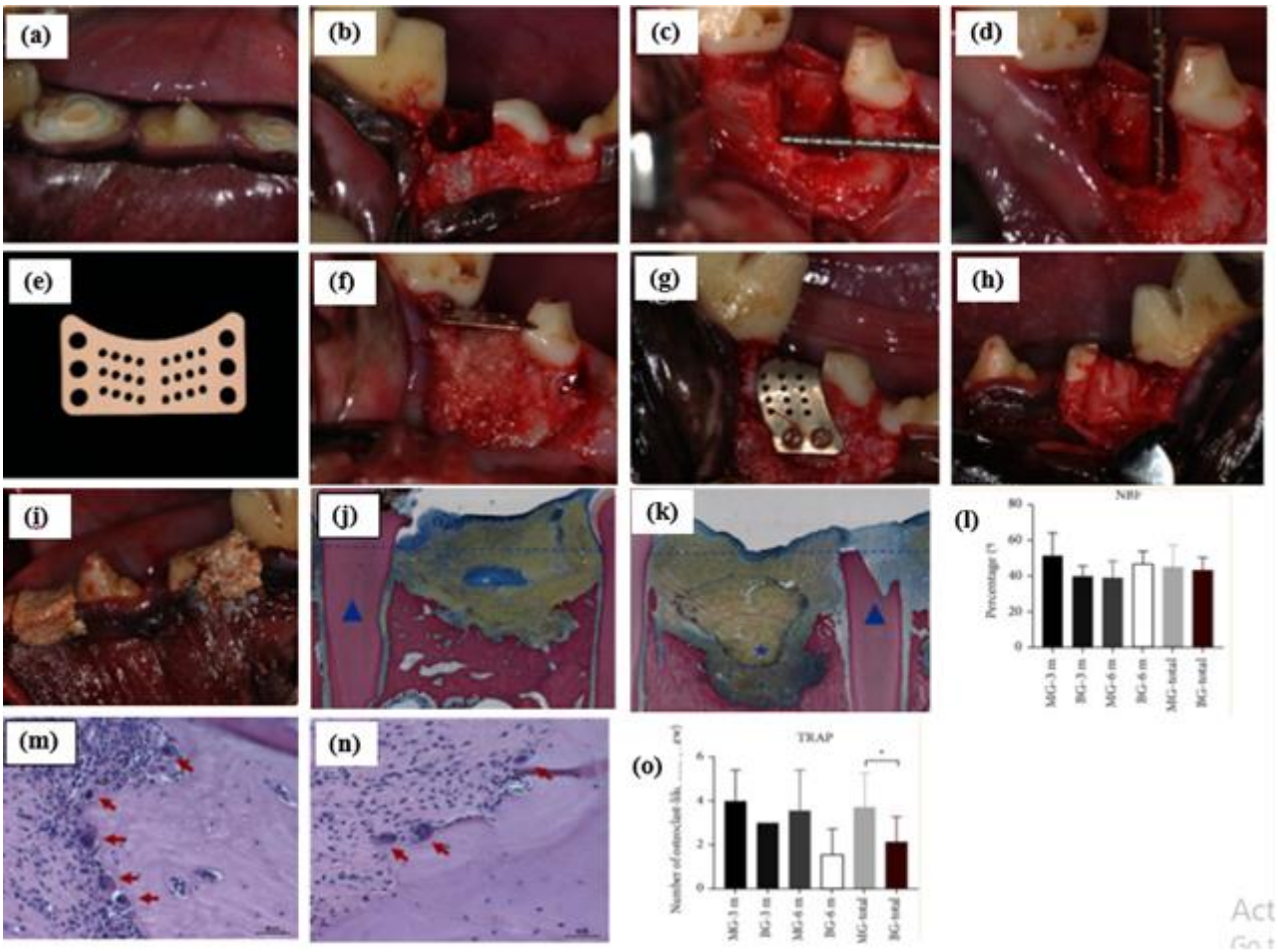


**Fig. 6: (a-i) Surgical procedure for DM grafting and applying MAR/Bio-Gide, (j-o) Quantitative Histological Assessment of Bone Formation [(j) group MG-3m, (k) group BG-3m), (m, n) TRAP-stained sections in MG-3m, and BG-3m groups, respectively. (i, o) The average number of TRAP for MG-3m and BG-3m groups, respectively [159].**

Wu et al. [160] conducted a study to improve the surface properties of pure magnesium mesh in order to reduce its degradation rate. The research focused on how this surface modification affects biodegradation and bone regeneration, particularly for guided bone regeneration (GBR) applications, using a critical-size defect model in rat calvaria. The two-step surface modification involved plasma electrolytic oxidation (PEO) followed by hydrothermal treatment (HT), resulting in

a protective layer primarily composed of $Mg(OH)_2$, containing approximately 8% phosphorus and measuring about 1 μm in thickness, as demonstrated by X-ray diffraction (XRD) results. After four weeks of implantation, the untreated magnesium mesh completely degraded, creating gas pockets between the mesh and the newly formed bone. These gas pockets, a byproduct of the degradation process, displaced surrounding tissues and impeded blood and body fluid supply, thereby hindering bone healing and promoting bone resorption. In contrast, the PEO/HT-treated magnesium mesh showed minimal degradation after the same period. Furthermore, new bone formation was observed along the surface of the treated mesh, extending from the edge of the base bone to the center of the defect. Over the 8-week implantation period, the untreated magnesium mesh fully degraded, and hydrogen gas evolution ceased. However, gas pockets were still observed emanating from the center of the treated magnesium mesh, attributed to localized corrosion caused by the breakdown of the PEO/HT coating. A key limitation of this study is its relatively short duration, highlighting the need for longer-term experiments to establish the complete duration necessary for full bone regeneration with magnesium.

## 4. Degradable 3D Scaffolds for Vertical Bone Augmentation

The advancement of three-dimensional biodegradable scaffolds for vertical bone augmentation is an ongoing area of research. Various biodegradable materials are employed in fabricating 3D scaffolds for bone augmentation.

### 4.1. Degradable Polymeric 3D Scaffold for Vertical Bone Augmentation

The flexibility and ductility of polymers utilized in creating 3D scaffolds enable them to conform to the shape of the defect and be securely affixed with titanium screws. Numerous studies in oro-dental tissue regeneration have explored the use of 3D-printed polymeric scaffolds [161, 162]. However, the translation of these efforts into clinical applications for vertical alveolar augmentation is still in progress. The significance of 3D polymeric scaffolds for vertical alveolar bone augmentation is underscored through various animal models. A noteworthy example involves the use of 3D polymeric (PCL)-TCP scaffolds, fabricated using fused deposition modeling techniques [163]. These scaffolds have demonstrated the facilitation of early revascularization and accelerated bone regeneration by either supporting seeded cells on the scaffold or allowing invading cells from the local host environment [23, 164, 165]. Additionally, PCL-TCP scaffolds have shown potential for enhancing mineralized tissue formation [166] and serving as a delivery system for platelet-rich plasma (PRP) and bone morphogenic protein [15, 167]. The PCL-TCP composite scaffold, characterized by high porosity (70–75%) and pore size exceeding 300 μm, proves suitable for hosting and facilitating the transfer of stem cells [167].

In a study conducted by Khojasteh et al [168], vertical bone augmentation was investigated using a 3D-printed β-TCP/PCL scaffold (20 × 10 × 10 $mm^3$). The research assessed the impact of a 3D-printed PCL/TCP scaffold infused with mesenchymal stem cells (MSCs) 24 hours before implantation on repairing a critical-sized vertical bone defect in a dog's mandible, with an 8-week healing period illustrated in Figure 7A-B. Results from the study highlight the superior performance of the cell-laden scaffold compared to the one without cell filling, as indicated by histomorphometric measurements detailed in Table 5. SEM micrograph analysis in Figure 7 (C–F) illustrates the dispersion of MSCs within the scaffold pores and their adhesion to the PCL-TCP scaffold. The authors attribute these outcomes to the bioinert nature of PCL, even when blended

with inorganic fillers. Notably, a prior study demonstrated the scaffold's secure fixation using a titanium screw, underscoring the resilience-enhancing properties of the PCL polymer block.

**Table 5: The Amount of new bone formation in the control and the test groups [168].**

| Test | Bone formation % | | Remaining Scaffold % | |
|---|---|---|---|---|
| | Control groups | MSCs containing groups | Control groups | MSCs containing groups |
| Mean ± SD | 17.27 ± 3.29 | 48.63 ± 4.66 | 36.55 ± 3.76 | 24.1 ± 4.13 |
| Minimum | 13.32 | 41.45 | 28.26 | 17.64 |
| Maximum | 24.45 | 55.78 | 40.12 | 30.21 |

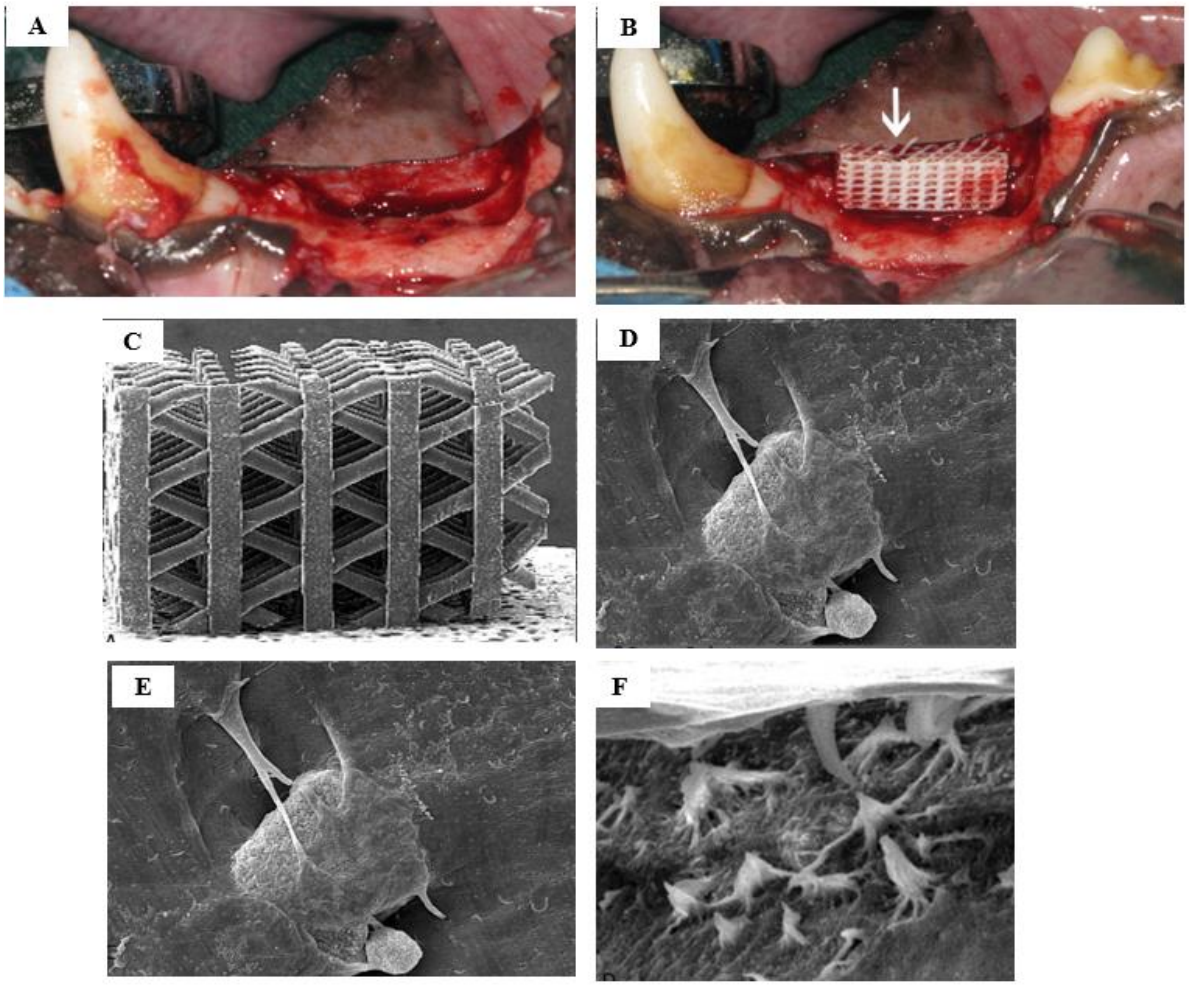


**Fig. 7: (A) Creating a critical-size vertical defect in the posterior mandible area of dogs; (B) fixation of the PCL-TCP blocks with a mini screw. C–F: SEM analysis of the PCL-TCP scaffold loaded with MSCs [(C) ×10)]. MSCs were entrapped in the porosity and attached to the walls [(D–F) ×1000] [168].**

Kumar et al. [169] investigated the potential of a biphasic PCL scaffold combined with a hyaluronic acid-based hydrogel containing BMP-2 for vertical bone regeneration in rabbits [33]. Using fused deposition modeling (FDM), they created 3D-printed biphasic scaffolds featuring an outer polymer shell that mimicked native cortical bone for mechanical support, while the interior resembled cancellous bone to enhance vascularization, as illustrated in Figure 8A. By employing PLLA domes during guided bone regeneration, they successfully prevented fibrous tissue infiltration. In their study, they examined the hydrogel-loaded BMP-2 within the scaffold using an extraskeletal lapine

model. They implemented a groove technique instead of transcortical perforations, which effectively reduced blood clot formation and delayed the initiation of the healing cascade, thereby influencing neovascularization and bone formation within the scaffold. The results indicated that the biphasic construct fulfilled the criteria for vertical bone augmentation, demonstrating both biomechanical stability and effective space maintenance. However, limited vertical bone formation was predominantly observed near the resident calvarial bone, as shown in Figure 8B-I (H&E). This limitation may be linked to insufficient vascularization post-implantation due to the surgical model employed.

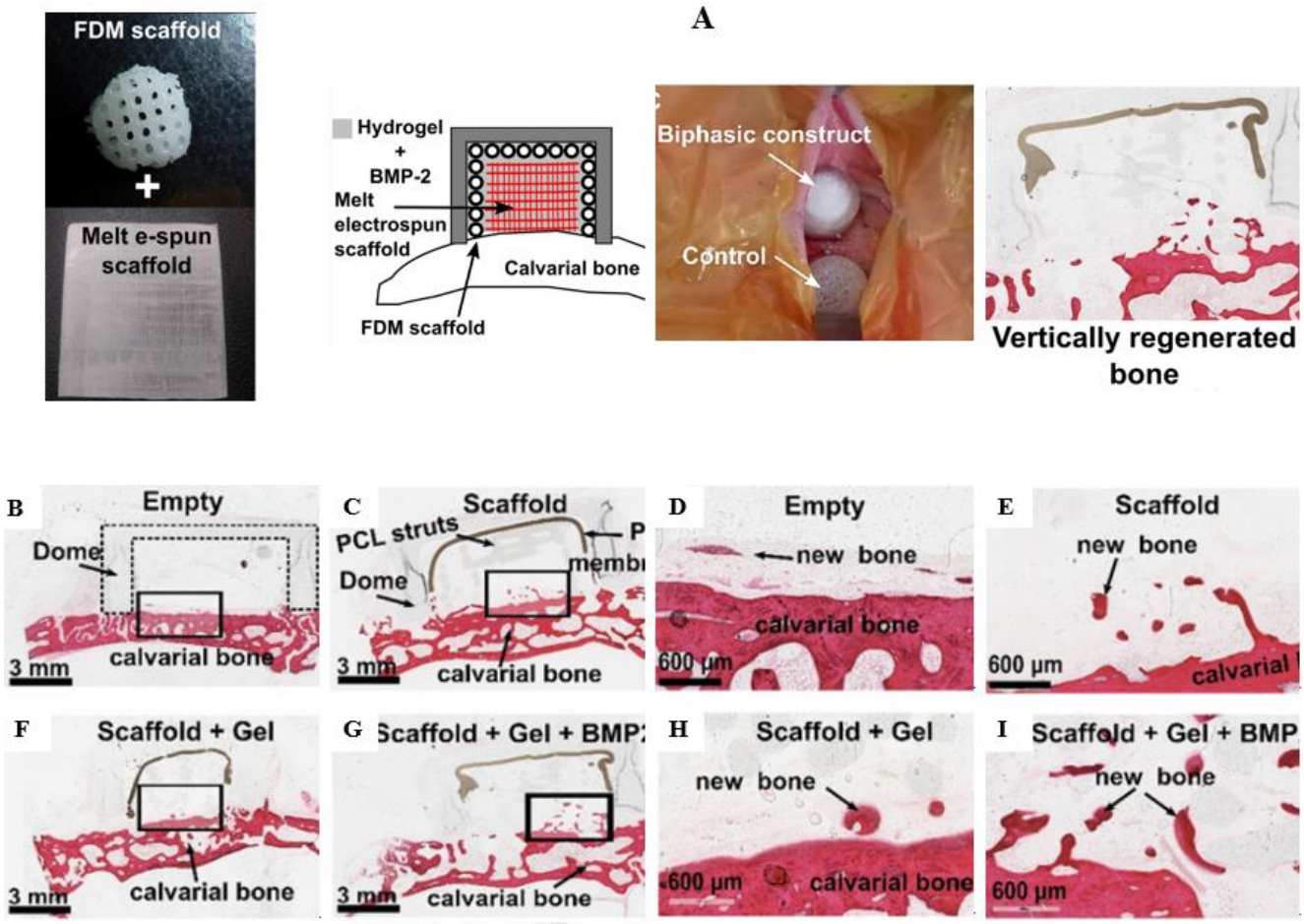


**Fig. 8: PCL biphasic scaffold loaded with hydrogel. (B-I) H& E-stained images. (B) PLLA dome, (C) PLLA dome combined with a biphasic scaffold. Magnified images for the empty dome (D) and the biphasic scaffold (E). (F) a PLLA dome combined with a biphasic scaffold and Hydrogel, (G) a PLLA dome combined with a biphasic scaffold, Hydrogel, and 30 µg BMP-2. (H) PLLA dome combined with a biphasic scaffold and composite Hydrogel, and (I) PLLA dome combined with a biphasic scaffold, composite hydrogel, and 30 µg BMP-2 [169].**

In a follow-up study using an extraskeletal ovine calvarium model, Vaquette et al. [11] assessed the efficacy of a PCL 3D-printed/melt-electrowritten biphasic scaffold for vertical bone augmentation. The study was conducted in two stages: the first stage focused on examining the effects of the scaffold and various BMP-2 dosages on bone formation, while the second stage evaluated bone maintenance and implant osseointegration through surgical re-entry and dental implant placement.
The experimental setups included an empty dome, a biphasic scaffold functionalized with a gelatin-hyaluronic hydrogel, and biphasic scaffolds functionalized with gelatin-hyaluronic hydrogel containing either 75 or 150 µg of BMP-2. Additionally, a gelatin-hyaluronic hydrogel alone or with BMP-2 at the same dosages was tested. Bone formation was observed exclusively in the elevated

space beneath the PLLA domes across all groups, with notably greater formation in the BMP-2-containing specimens, as illustrated in the three-dimensional reconstructions of CT scans and bone volume quantifications in Figure 9A-G.

Results from the first stage indicated that the scaffold enhanced vertical bone augmentation due to its capacity to retain the hydrogel. However, BMP-2 dosage did not significantly affect the volume of extraskeletal-formed bone, suggesting a threshold dose necessary to initiate bone formation in a given defect volume.

In the second stage, dental implants were placed in the bone formed by the BMP-2-containing hydrogel or the BMP-2-functionalized biphasic scaffold after an 8-week healing period post-implantation. Bone resorption was noted in the absence of a biphasic scaffold, as depicted in Figure 9H-N. These findings demonstrate that a long-term space-maintaining scaffold can prevent early bone resorption and provide enhanced dimensional stability to the elevated bone. Given that PCL has a very slow degradation rate (spanning 3 to 5 years), a longer healing period is essential to determine whether the elevated bone can be maintained over extended durations after the complete degradation of the PCL scaffold [170, 171].

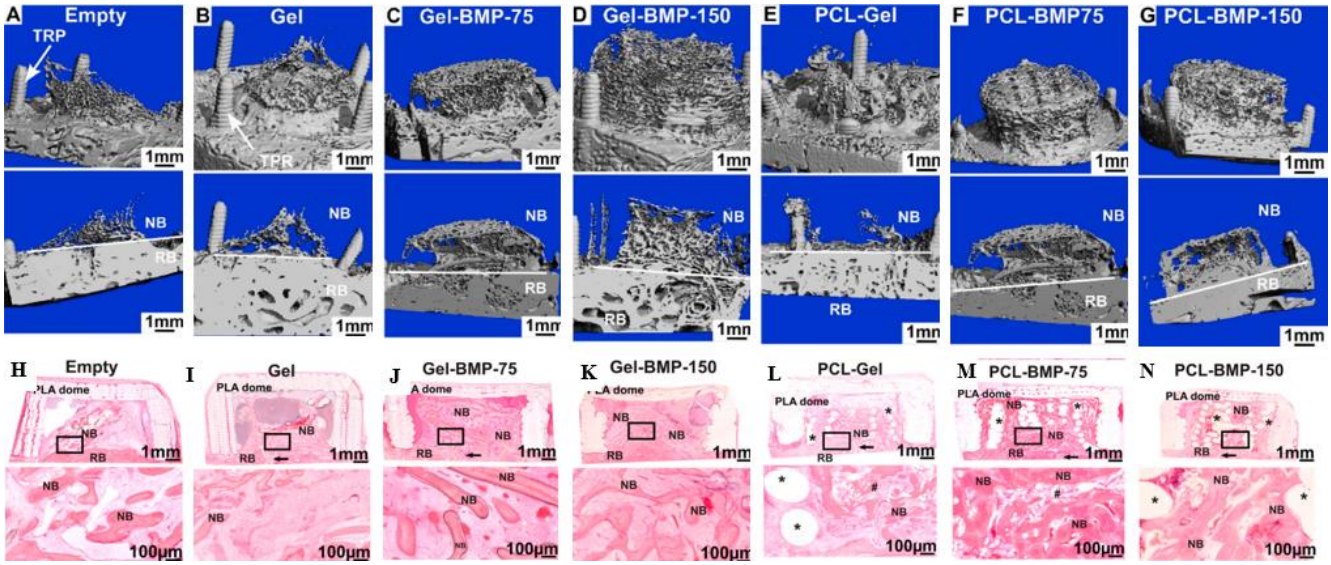


**Fig. 9: (A-G) Micro-computed tomography of bone volume. NB denotes new bone, and RB denotes resident bone. (H-N) Histological (H&E) and histomorphometric assessment of bone formation at 8 weeks post-implantation [11].**

In a preliminary clinical study, Goh et al. [172] evaluated the feasibility and effectiveness of a 3D-printed PCL scaffold designed to maintain space in fresh extraction sockets during ridge preservation. The study involved thirteen patients, with six receiving the PCL scaffold in the extraction socket and seven acting as a control group without any space filler. Following a six-month post-surgery period, micro-CT and histological analyses of a central bone segment were conducted to assess newly formed bone. The findings revealed that patients who received the 3D scaffold experienced significantly greater bone height compared to those in the control group. This superior outcome was linked to the low degradation rate of the PCL polymer during the first six months post-surgery. While both groups exhibited some degree of bone ridge resorption, the PCL scaffold helped to mitigate this process by preserving its geometry during the initial healing phase. However, despite its benefits for immediate space preservation, the scaffold's lack of material resorption could hinder new bone formation, potentially affecting the long-term success of the ridge preservation procedure.

Farag et al. [173] explored a multifunctional biphasic PCL 3D scaffold (250 μm pore size) using a melt electrowetting (MEW) device, modifying its surface with calcium phosphate nano-plates/flakes for periodontal regeneration. They created decellularized tissue-engineered constructs (TEC) by seeding human osteoblasts (hOBs) within the coated 3D scaffold for a 28-day study, guiding tissue-specific cellular repopulation. The biphasic construct included an in vitro periodontal ligament (PDL) cell sheet on the bone compartment's surface. The study also assessed lyophilization's role in preserving biphasic TEC for periodontal regeneration. The scaffold replicated the natural bone extracellular matrix (ECM) with adequate porosity for cell movement and nutrient exchange. SEM analysis showed well-preserved PCL fiber morphology, with a CaP layer forming after soaking in HBSS. This CaP coating, maintaining its nanostructure through decellularization and lyophilization, demonstrated effective ECM preservation in both PDL and bone compartments. The condensed ECM morphology in the PDL compartment suggested lyophilization's crosslinking effect, contrasting with a well-preserved decellularized matrix without lyophilization.

### 4.2. Degradable Biometallic 3D Scaffolds for Vertical Bone Augmentation

Titanium and titanium alloys are considered crucial biometallic materials due to their exceptional biocompatibility, excellent mechanical properties, and elasticity [165]. Their favorable characteristics make them highly suitable for various bone regeneration applications. Titanium-based 3D scaffolds, known for good hydrophilicity, facilitate mineral deposition, cell attachment, and proliferation in vitro [165]. They promote the formation of new bones in vivo without causing inflammation or necrosis around the implant sites [174]. Despite these advantages, the issue of permanent implants has led to the exploration of biodegradable metallic alloys.

Creating 3D magnesium scaffolds is possible through various techniques, such as powder metallurgy, laser etching, and rapid prototyping. Powder bed fusion (PBF), using laser (L-PBF) or electron beam (EB-PBF), is a commonly used technique for producing metallic implants. However, challenges arise with magnesium because of its high chemical reactivity and evaporation during the PBF process. Magnesium-based metals cannot be melted using EB-PBF, as the evaporation products interfere with the electron beam's propagation in a vacuum [175]. Laser etching techniques, while capable of producing 3D magnesium scaffolds with high porosity and well-distributed pore size, face challenges due to magnesium's high affinity to oxygen and low boiling temperature [176]. Innovative scaffold materials with appropriate properties for bone applications are being developed to address fabrication method drawbacks for Mg scaffolds, including uneven pore distribution, residue induction, and high-tech expenses. One such technique is fiber deposition hot pressing (FDHP) technology, introduced by Zhang et al. to produce a novel 3D porous Mg scaffold [177] as illustrated in Figure 10A. The study revealed that the pores are evenly distributed on the magnesium scaffold's surface, with rectangular shapes regardless of the sample direction. Figure 10 (B)–(D) indicates that the size of one type of pore (axial pore) is controlled by the fiber distribution, while the size of the other type (lateral pore) is determined by the fiber height, as shown in Figure 10(E)–(G).

Lin et al [178] utilized 3DGP to fabricate porous Mg scaffolds and implanted them into the femoral condyle of rats to evaluate their bone regeneration potential. The scaffolds were designed with a porosity of 60-80% and interconnected pores ranging from 100 to 300 μm, which are considered optimal for bone tissue ingrowth [179]. The results showed that the Mg scaffolds exhibited good biocompatibility and supported new bone formation within the pores. Histological analysis revealed osteoblasts and new bone matrix, indicating that the scaffolds provided a favorable environment for bone regeneration.

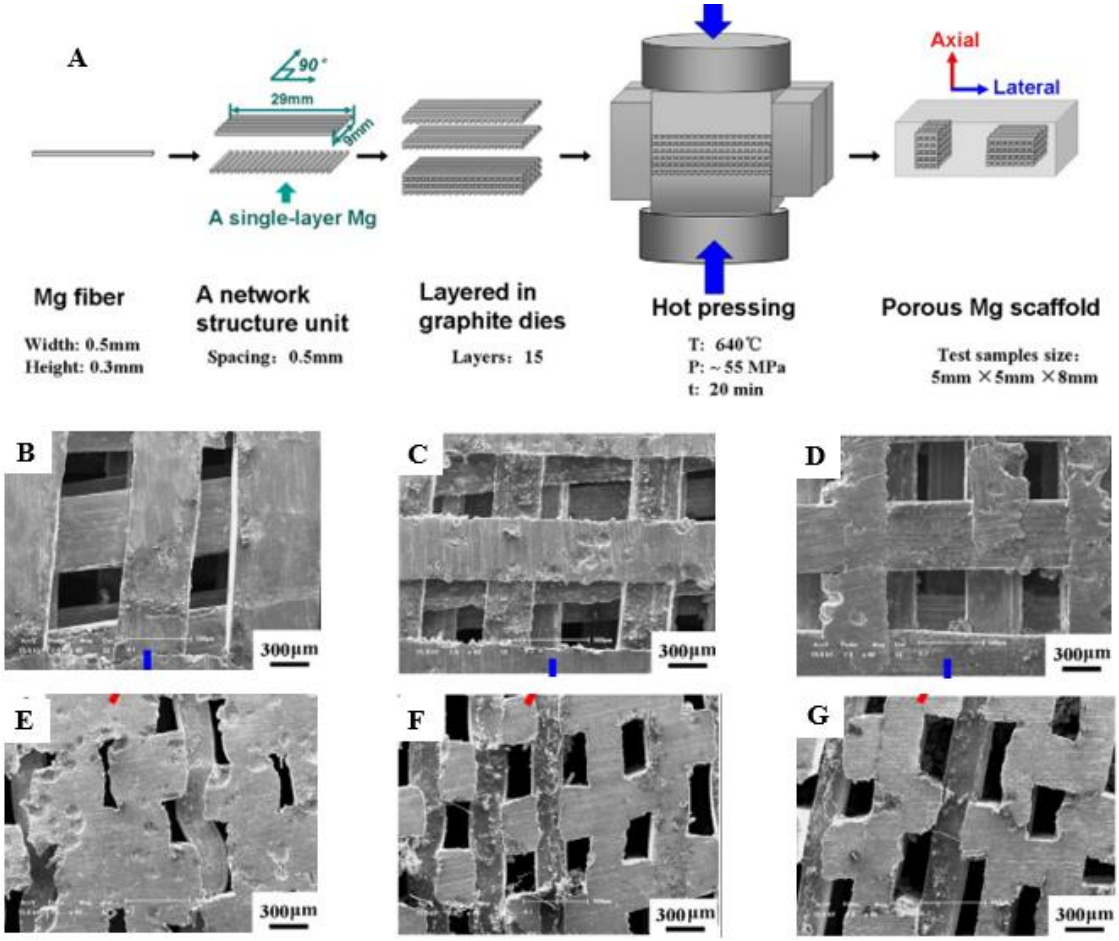


**Fig. 10: B-G) SEM micrographs of two kinds of pores on the surface of axial porous Mg samples with porosity ranging from 33% to 54%. B, C, and D axial direction with porosity of 33%, 48%, and 54 % respectively; E, F, and G lateral direction with porosity of 33%, 48%, and 54 % respectively [177].**

Wang et al. [180] employed Fused Deposition Modeling (FDM) to create a PCL/Zn 3D composite scaffold with varying Zn powder contents (1 wt.%, 2 wt.%, and 3 wt.%). The study comprehensively evaluated the mechanical properties, cytocompatibility, Zn ion release behavior in vitro, and osteogenesis and osteoclastogenesis features in a rat model of calvaria defects for the produced PCL/Zn scaffolds. Notably, the addition of Zn powder enhanced the mechanical properties, although excessive Zn particles impacted the integrity of the PCL fiber. Due to PCL's inherent hydrophobic nature, contact angle measurements demonstrated increased scaffold hydrophilicity with rising Zn content, aligning with a related study incorporating magnesium particles into a PCL scaffold. [181]. The contact angle measurements demonstrated that the hydrophilicity of the scaffold increased with increasing Zn content, and these findings supported those of a related study reported by Zhao et al, when they incorporated magnesium particles into a PCL scaffold [182]. These changes were attributed to the hydrophilic nature of metal powders compared to pure PCL and alterations in PCL surface structure during extrusion and molding. Although no scaffolds exhibited apparent cytotoxicity, those with 2 wt% and 3 wt% Zn showed increased cell adhesion on the surfaces, consistent with hydrophilicity results. The in vivo bone formation-promoting effect of Zn was dose-dependent. Eight weeks post-implantation, Zn powder addition promoted new bone formation across all scaffold-containing groups compared to the blank control. The PCL scaffold with 2 wt% Zn exhibited the most favorable osteogenic effect on bone formation. However, concentration increases to 3 wt% Zn led to a significant rise in osteoclasts at the new bone tissue edge, resulting in decreased new bone formation. This study provides valuable

insights into Zn's role in bone regeneration, highlighting its potential for endowing composite materials with enhanced biological functions.

## 5. Prospects and Future Directions

The future of vertical bone augmentation is being revolutionized by the combination of additive manufacturing and biodegradable scaffolds. This technology is moving beyond simply creating custom-shaped, bone-guiding structures and is instead advancing towards the development of dynamic, "4D" systems [183]. These next-generation scaffolds are designed to change over time within the body, capable of transforming from a compact shape for minimal surgical invasion into a complex structure or of releasing growth factors on demand in response to specific biological signals [184]. This evolution from a passive implant to an active participant allows for a more precise and sophisticated healing process.

To further mimic natural bone, research is focusing on multi-material printing that creates scaffolds with graded properties, transitioning from a dense exterior to a porous interior, just like real bone [185]. A critical parallel goal is ensuring these constructs rapidly develop blood vessels. The strategy is shifting from merely placing cells on a scaffold to pre-printing them into functional micro-tissues [186]. By precisely arranging a patient's stem cells and blood vessel-forming cells together, surgeons can implant a scaffold that already contains a pre-formed network of capillaries [187]. Through this collaborative effort across scientific disciplines, the goal of reliably regenerating complex bone defects is becoming an achievable reality, heralding a new era of personalized regenerative medicine.

## 6. Conclusions

This review highlighted guided bone regeneration in vertical augmentation and recent progress in additive manufacturing of biodegradable membranes and scaffolds. These structures, crafted from biodegradable polymeric and metallic materials, represent a promising frontier in the field of vertical bone augmentation. The central focus of this review was on the progress achieved through the utilization of biodegradable membranes and 3D scaffolds for vertical bone augmentation. Notably, the demand for patient-specific geometries emerges as an important consideration for the future of this field. Crafting anatomically precise builds is imperative, as it not only facilitates the generation of extraskeletal bone but also ensures long-term space maintenance. This, in turn, enables multiple cycles of bone remodeling, ultimately curbing bone resorption post-implant insertion and thereby enhancing the durability of implants. Despite the strides made, several technical challenges persist. The optimization of manufacturing processes for enhanced precision, the development of advanced biomaterials with improved biomechanical properties, and the establishment of standardized protocols for clinical implementation remain key hurdles. Future opportunities lie in the continued integration of cutting-edge nanotechnologies to tailor implants to individual patient needs, thereby ushering in an era of personalized regenerative medicine.

## 7. References

[1] A. Shakya, Y. Li, N.-w. Chang, X. Liu, Supra-alveolar bone regeneration: progress, challenges, and future perspectives, Composites Part B: Engineering (2024) 111673.

[2] A. Pabst, J. Wiegner, M. Schneider, N. Weyer, A. Bartella, M. Heiland, P. Becker, A.-N. Zeller, Alveolar ridge augmentation in Oral and Maxillofacial Surgery: a study on current practices, patient management and innovations in Germany, International Journal of Implant Dentistry 11(1) (2025) 31.

[3] M. Sadat-Shojai, M. Asadnia, M.B. Shahsavani, M.M. Yousefi, Bone regenerative medicine: An emerging field with opportunities and challenges, Journal of the American Ceramic Society (2025) e20508.

[4] A. Raj, S. Pradhan, P. Shetty, D. Kadakampally, N. Shetty, Comparison of crestal bone loss and papilla fill after conventional and immediate implant placement: A 12 month clinical and radiographic prospective study, F1000Research 12 (2024) 821.

[5] E. Couso-Queiruga, Z.A. Graham, T. Peter, O. Gonzalez-Martin, P. Galindo-Moreno, G. Avila-Ortiz, Effect of periodontal phenotype characteristics on post-extraction dimensional changes of the alveolar ridge: A prospective case series, Journal of clinical periodontology 50(5) (2023) 694-706.

[6] N. De Angelis, Z.H. Kassim, E. Mohd Yusof, C. Yumang, M. Menini, Bone Augmentation Techniques with Customized Titanium Meshes: A Systematic Review of Randomized Clinical Trials, The Open Dentistry Journal 17(1) (2023).

[7] I.A. Urban, E. Montero, A. Monje, I. Sanz-Sánchez, Effectiveness of vertical ridge augmentation interventions: A systematic review and meta-analysis, Journal of Clinical Periodontology 46 (2019) 319-339.

[8] M. Moussa, J.-P. Carrel, S. Scherrer, M. Cattani-Lorente, A. Wiskott, S. Durual, Medium-term function of a 3D printed TCP/HA structure as a new osteoconductive scaffold for vertical bone augmentation: A simulation by BMP-2 activation, Materials 8(5) (2015) 2174-2190.

[9] J.P. Carrel, A. Wiskott, S. Scherrer, S. Durual, Large bone vertical augmentation using a three-dimensional printed TCP/HA bone graft: A pilot study in dog mandible, Clinical implant dentistry and related research 18(6) (2016) 1183-1192.

[10] J.P. Carrel, A. Wiskott, M. Moussa, P. Rieder, S. Scherrer, S. Durual, A 3D printed TCP/HA structure as a new osteoconductive scaffold for vertical bone augmentation, Clinical Oral Implants Research 27(1) (2016) 55-62.

[11] C. Vaquette, J. Mitchell, T. Fernandez-Medina, S. Kumar, S. Ivanovski, Resorbable additively manufactured scaffold imparts dimensional stability to extraskeletally regenerated bone, Biomaterials 269 (2021) 120671.

[12] A. Abdal-hay, M. Bartnikowski, F. Blaudez, C. Vaquette, D.W. Hutmacher, S. Ivanovski, Unique uniformity of calcium phosphate nanoparticle distribution in polymer substrates for additive manufacturing, Composites Part A: Applied Science and Manufacturing 173 (2023) 107670.

[13] A. Abdal-hay, F.A. Sheikh, N. Gómez-Cerezo, A. Alneairi, M. Luqman, H.R. Pant, S. Ivanovski, A review of protein adsorption and bioactivity characteristics of poly ε-caprolactone scaffolds in regenerative medicine, Eur. Polym. J. 162 (2022) 110892.

[14] L. Polo-Corrales, M. Latorre-Esteves, J.E. Ramirez-Vick, Scaffold design for bone regeneration, Journal of nanoscience and nanotechnology 14(1) (2014) 15-56.

[15] X. Wei, W. Zhou, Z. Tang, H. Wu, Y. Liu, H. Dong, N. Wang, H. Huang, S. Bao, L. Shi, Magnesium surface-activated 3D printed porous PEEK scaffolds for in vivo osseointegration by promoting angiogenesis and osteogenesis, Bioactive Materials 20 (2023) 16-28.

[16] T.-F. Valamvanos, X. Dereka, H. Katifelis, M. Gazouli, N. Lagopati, Recent advances in scaffolds for guided bone regeneration, Biomimetics 9(3) (2024) 153.

[17] R. De Pace, S. Molinari, E. Mazzoni, G. Perale, Bone regeneration: A review of current treatment strategies, Journal of Clinical Medicine 14(6) (2025) 1838.

[18] S. Kim, S.-G. Kim, Advancements in alveolar bone grafting and ridge preservation: a narrative review on materials, techniques, and clinical outcomes, Maxillofacial Plastic and Reconstructive Surgery 46(1) (2024) 14.

[19] S. Sassi, T. Watanabe, T. Shinoka, Scaffold and Cell-Based Tissue Engineering Approaches as Alternative Therapy for Blood Vessel Disease, (2023).

[20] E. Rosellini, M.G. Cascone, Microfluidic Fabrication of Natural Polymer-Based Scaffolds for Tissue Engineering Applications: A Review, Biomimetics 8(1) (2023) 74.

[21] C. Xu, Z. Liu, X. Chen, Y. Gao, W. Wang, X. Zhuang, H. Zhang, X. Dong, Bone tissue engineering scaffold materials: Fundamentals, advances, and challenges, Chinese Chemical Letters (2023) 109197.

[22] S. Vach Agocsova, M. Culenova, I. Birova, L. Omanikova, B. Moncmanova, L. Danisovic, S. Ziaran, D. Bakos, P. Alexy, Resorbable Biomaterials Used for 3D Scaffolds in Tissue Engineering: A Review, Materials 16(12) (2023) 4267.

[23] L. Suamte, A. Tirkey, J. Barman, P.J. Babu, Various manufacturing methods and ideal properties of scaffolds for tissue engineering applications, Smart Materials in Manufacturing 1 (2023) 100011.

[24] M.V. Deshpande, A. Girase, M.W. King, Degradation of Poly (ε-caprolactone) Resorbable Multifilament Yarn under Physiological Conditions, Polymers 15(18) (2023) 3819.

[25] J.Y. Shi, E. Montero, X.Y. Wu, D. Palombo, S.M. Wei, I. Sanz-Sánchez, Bone preservation or augmentation simultaneous with or prior to dental implant placement: A systematic review of outcomes and outcome measures used in clinical trials in the last 10 years, Clinical Oral Implants Research 34 (2023) 68-83.

[26] Z. Sheikh, C. Sima, M. Glogauer, Bone replacement materials and techniques used for achieving vertical alveolar bone augmentation, Materials 8(6) (2015) 2953-2993.

[27] V.A. Georgeanu, O. Gingu, I.V. Antoniac, H.O. Manolea, Current options and future perspectives on bone graft and biomaterials substitutes for bone repair, from clinical needs to advanced biomaterials research, Applied Sciences 13(14) (2023) 8471.

[28] M. Zhou, Y. Ma, X. Jia, Y. Wu, J. Liu, Y. Wang, P. Wang, J. Luo, F. Lin, J. Wang, Comparison of free vascularized fibular grafts and the Masquelet technique for the treatment of segmental bone defects with open forearm fractures: a retrospective cohort st udy, Journal of Orthopaedics and Traumatology 25(1) (2024) 44.

[29] A. Picone, F. Castro, A. Falcão, J.G. Medina, E. Minetti, J.C.H. Fernandes, G.V.O. Fernandes, Autogenous Tooth Graft Biomaterial in Guided Bone Regeneration: A Comprehensive Review, Surgeries 5(4) (2024) 929-947.

[30] J. Narde, D. Ganapathy, K.K. Pandurangan, Evaluation of the Success of Autogenous Block Grafting in Atrophic Maxillary and Mandibular Ridges Prior to and After Implant Placement, Cureus 16(2) (2024).

[31] S. Olate, F. Uribe, C. Huentequeo-Molina, D.R. Goulart, E.A. Sigua-Rodriguez, J.P. Alister, Mandibular angle contouring using porous polyethylene stock or PEEK-based patient specific implants. A critical analysis, Journal of Craniofacial Surgery 32(1) (2021) 242-246.

[32] A. Abouchenari, N. Tajbakhsh, A. Shahbaz, G. Alamdari-Mahd, Advancements in dental implant technology: the impact of smart polymers utilized through 3D printing, Journal of synthesis and sintering 4(2) (2024).

[33] F. Ali, S.N. Kalva, M. Koc, Advancements in 3D printing techniques for biomedical applications: A comprehensive review of materials consideration, post processing, applications, and challenges, Discover Materials 4(1) (2024) 53.

[34] M. Mirshafiei, H. Rashedi, F. Yazdian, A. Rahdar, F. Baino, Advancements in tissue and organ 3D bioprinting: Current techniques, applications, and future perspectives, Materials & Design (2024) 112853.

[35] F. Muddebihal, R.G.A. Veetil, S.M.A. Feroz, R.S. Saini, S.S. Khan, R.S. Preethanath, J.S. Babu, C. Swarnalatha, A.S. Nayyar, Guided bone regeneration-assisted bone augmentation and early implant placement protocols: A case report, Journal of Clinical Sciences 22(1) (2025) 51-56.

[36] E. Rosen, I. Tsesis, E. Kavalerchik, R. Salem, A. Kahn, M. Del Fabbro, S. Taschieri, S. Corbella, Effect of Guided Tissue Regeneration on the Success of Surgical Endodontic Treatment of Teeth with Endodontic-Periodontal Lesions: a Systematic Review, International Endodontic Journal (2023).

[37] I.A. Urban, E. Montero, E. Amerio, D. Palombo, A. Monje, Techniques on vertical ridge augmentation: Indications and effectiveness, Periodontology 2000 (2023).

[38] F. Shiezadeh, H.R. Arab, V. Khoshkam, A. Moeintaghavi, A. Forouzanfar, L. Khodadadifard, Comparison of Guided Bone Regeneration with Periosteal Pocket Flap Technique Versus Autogenous Bone Block Graft for Horizontal Bone Augmentation: A Clinical Trial Study, International Journal of Periodontics & Restorative Dentistry 43(4) (2023).

[39] A. Monje, A. Roccuzzo, D. Buser, H.L. Wang, Influence of buccal bone wall thickness on the peri-implant hard and soft tissue dimensional changes: A systematic review, Clinical oral implants research 34(3) (2023) 157-176.

[40] A.M. Alqahtani, Guided Tissue and Bone Regeneration Membranes: A Review of Biomaterials and Techniques for Periodontal Treatments, Polymers 15(16) (2023) 3355.

[41] R. Noelken, B. Al-Nawas, Bone regeneration as treatment of peri-implant disease: A narrative review, Clinical Implant Dentistry and Related Research (2023).

[42] G. Ma, C. Wu, M. Shao, Simultaneous implant placement with autogenous onlay bone grafts: a systematic review and meta-analysis, International Journal of Implant Dentistry 7(1) (2021) 1-11.

[43] G. Kumar, H. Parthasarathy, D. Ponnaiyan, Localized ridge augmentation with simultaneous implant placement followed by soft tissue augmentation in the maxillary anterior region: A case report, World Academy of Sciences Journal 4(5) (2022) 1-6.

[44] L. Sbricoli, R. Guazzo, M. Annunziata, L. Gobbato, E. Bressan, L. Nastri, Selection of collagen membranes for bone regeneration: A literature review, Materials 13(3) (2020) 786.

[45] M. Laubach, F. Hildebrand, S. Suresh, M. Wagels, P. Kobbe, F. Gilbert, U. Kneser, B.M. Holzapfel, D.W. Hutmacher, The concept of scaffold-guided bone regeneration for the treatment of long bone defects: current clinical application and future perspective, Journal of Functional Biomaterials 14(7) (2023) 341.

[46] J.-K. Ku, Y.-K. Kim, P.-Y. Yun, Influence of biodegradable polymer membrane on new bone formation and biodegradation of biphasic bone substitutes: An animal mandibular defect model study, Maxil lofacial plastic and reconstructive surgery 42(1) (2020) 1-7.

[47] R. Nahid, M. Bansal, S. Pandey, Horizontal bone augmentation using two membranes at dehisced implant sites: A randomized clinical study, Journal of Oral Biology and Craniofacial Research 12(5) (2022) 487-491.

[48] M.M.-S. Antón, F. Pérez-González, C. Meniz-García, Titanium mesh for guided bone regeneration: a systematic review, British Journal of Oral and Maxillofacial Surgery (2024).

[49] Z. Yang, C. Wu, H. Shi, X. Luo, H. Sun, Q. Wang, D. Zhang, Advances in barrier membranes for guided bone regeneration techniques, Frontiers in bioengineering and biotechnology 10 (2022) 921576.

[50] H. Wosicka-Frąckowiak, K. Poniedziałek, S. Woźny, M. Kuprianowicz, M. Nyga, B. Jadach, B. Milanowski, Collagen and its derivatives serving biomedical purposes: a review, Polymers 16(18) (2024) 2668.

[51] S. Patil, S. Bhandi, M.M.H. Bakri, D.H. Albar, K.J. Alzahrani, M.S. Al-Ghamdi, M.M. Alnfiai, M.R. Tovani-Palone, Evaluation of efficacy of non-resorbable membranes compared to resorbable membranes in patients undergoing guided bone regeneration, Heliyon (2023).

[52] J.-C. Song, J. Suwanprateeb, D. Sae-Lee, T. Sosakul, S. Kositbowornchai, P. Klanrit, W. Pitiphat, S. Prajaneh, Clinical and histological evaluations of alveolar ridge augmentation using a novel bi-layered porous polyethylene barrier membrane, Journal of Oral Science 62(3) (2020) 308-313.

[53] G.L. Abe, J.I. Sasaki, R. Tsuboi, T. Kohno, H. Kitagawa, S. Imazato, Poly (lactic acid/caprolactone) bilayer membrane achieves bone regeneration through a prolonged barrier function, Journal of Biomedical Material
s Research Part B: Applied Biomaterials 112(1) (2024) e35365.

[54] Y.D. Rakhmatia, Y. Ayukawa, A. Furuhashi, K. Koyano, Current barrier membranes: titanium mesh and other membranes for guided bone regeneration in dental applications, Journal of prosthodontic research 57(1) (2013) 3-14.

[55] M. Toledano-Osorio, M. Toledano, F.J. Manzano-Moreno, C. Vallecillo, M. Vallecillo-Rivas, A. Rodriguez-Archilla, R. Osorio, Alveolar bone ridge augmentation using polymeric membranes: A systematic review and meta-analysis, Polymers 13(7) (2021) 1172.

[56] M.A. Aladmawy, Z.S. Natto, M. Kreitzer, Y. Ogata, Y. Hur, Histological and histomorphometric evaluation of alveolar ridge preservation using an allograft and nonresorbable membrane with and without primary closure: a pilot randomized controlled clinic
al trial, Medicine 101(26) (2022).

[57] S. Martins, F. Poblete, A. Braga, L. de Lima Sousa, D. Bordin, Vertical Ridge Augmentation of Edentulous Posterior Inferior Jaw Using Lumina Bone Porous Large®: A Clinical Case Report, J Dent Oral Sci 3(3) (2021) 1-6.

[58] A. Friedmann, W. Goetz, Composite block sponge proved facilitating bone augmentation, Clinical Oral Implants Research 31 (2020) 159-159.

[59] M.M.a. Imran, A. Che Idris, L.C. De Silva, Y.-B. Kim, P.E. Abas, Advancements in 3D printing: Directed energy deposition techniques, defect analysis, and quality monitoring, Technologies 12(6) (2024) 86.

[60] I. Fidan, O. Huseynov, M.A. Ali, S. Alkunte, M. Rajeshirke, A. Gupta, S. Hasanov, K. Tantawi, E. Yasa, O. Yilmaz, Recent inventions in additive manufacturing: Holistic review, Inventions 8(4) (2023) 103.

[61] E. Davoodi, H. Montazerian, A.S. Mirhakimi, M. Zhianmanesh, O. Ibhadode, S.I. Shahabad, R. Esmaeilizadeh, E. Sarikhani, S. Toorandaz, S.A. Sarabi, Additively manufactured metallic biomaterials, Bioactive Materials 15 (2022) 214-249.

[62] K. Hayashi, M. Shimabukuro, R. Kishida, A. Tsuchiya, K. Ishikawa, Structurally optimized honeycomb scaffolds with outstanding ability for vertical bone augmentation, Journal of Advanced Research 41 (2022) 101-112.

[63] C.S. Choy, W.F. Lee, P.Y. Lin, Y.-F. Wu, H.-M. Huang, N.-C. Teng, Y.-H. Pan, E. Salamanca, W.-J. Chang, Surface Modified β-Tricalcium phosphate enhanced stem cell osteogenic differentiation in vitro and bone regeneration in vivo, Scientific Reports 11(1) (2021) 9234.

[64] E. Salamanca, Y.-H. Pan, Y.-S. Sun, H.-W. Hsueh, O. Dorj, W.-L. Yao, J.C.-Y. Lin, N.-C. Teng, I. Watanabe, S. Abe, Magnesium modified β-tricalcium phosphate induces cell osteogenic differentiation in vitro and bone regeneration in viv
o, International journal of molecular sciences 23(3) (2022) 1717.

[65] M. Hao, L. Xue, X. Wen, L. Sun, L. Zhang, K. Xing, X. Hu, J. Xu, D. Xing, Advancing bone regeneration: unveiling the potential of 3D cell models in the evaluation of bone regenerative materials, Acta Biomaterialia (2024).

[66] Y. Deng, Y. Liang, X. Liu, Biomaterials for Periodontal Regeneration, Dental Clinics 66(4) (2022) 659-672.

[67] A. Abdal-Hay, N.A. Kocak-Oztug, F.A. Sheikh, P. Han, S. Anwar, B.P. Fournier, S. Ivanovski, Fabrication of 3D bioactive melt electrowriting composite scaffold with high osteogenic potential, Colloids and Surfaces B: Biointerfaces 245 (2025) 114270.

[68] C. Ghayor, I. Bhattacharya, F.E. Weber, The optimal microarchitecture of 3D-printed β-TCP bone substitutes for vertical bone augmentation differs from that for osteoconduction, Materials & Design 204 (2021) 109650.

[69] M. Monstaporn, C. Rungsiyakull, W. Jia-mahasap, N. Pleumsamran, A. Mahrous, P. Rungsiyakull, Effects of bone types on bone remodeling of a dental implant: a review of the literature, Chiang Mai Dental Journal (CMDJ) 42(2) (2021) 14-17.

[70] Y. Kinoshita, H. Maeda, Recent developments of functional scaffolds for craniomaxillofacial bone tissue engineering applications, The Scientific World Journal 2013 (2013).

[71] J. Ye, X. Zhou, Z. Huang, X. Zhang, W. Huang, B. Wu, H. Zhou, Low-temperature-field-assisted fabrication of cross-scale tissue engineering scaffolds, International Journal of Extreme Manufacturing 7(2) (2024) 022011.

[72] M. Aftab, S. Ikram, M. Ullah, N. Khan, M. Naeem, M.A. Khan, R.B. Bakhtiyor o'g'li, K.S.S. Qizi, O.O. Erkinjon Ugli, B.M. Abdurasulovna, Recent Trends and Future Directions in 3D Printing of Biocompatible Polymers, Journal of Manufacturing and Materials Processing 9(4) (2025) 129.

[73] T. Ramos, L. Moroni, Tissue engineering and regenerative medicine 2019: the role of biofabrication—a year in review, Tissue Engineering Part C: Methods 26(2) (2020) 91-106.

[74] M.M. Farag, Z.M. Al-Rashidy, Methods Used to Fabricate Tissue Engineering Scaffolds, Biomaterials for Tissue Regeneration: Advances and Challenges for Fabrication and Clinical Translation, Springer2024, pp. 39-57.

[75] P. Brahme, N. Rarokar, R. Kumbhalkar, S. Saoji, P. Khedekar, Natural and synthetic polymeric hydrogel: a bioink for 3D bioprinting of tissue models, Journal of Drug Delivery Science and Technology (2024) 106204.

[76] J.L. Cota Quintero, R. Ramos-Payán, J.G. Romero-Quintana, A. Ayala-Ham, M. Bermúdez, E.M. Aguilar-Medina, Hydrogel-Based Scaffolds: Advancing Bone Regeneration Through Tissue Engineering, Gels 11(3) (2025) 175.

[77] Y. Delkash, M. Gouin, T. Rimbeault, F. Mohabatpour, P. Papagerakis, S. Maw, X. Chen, Bioprinting and in vitro characterization of an eggwhite-based cell-laden patch for endothelialized tissue

engineering applications, Journal of Functional Biomaterials 12(3) (2021) 45.
[78] Y. Wang, C. Lin, Study on properties of 3D-printed GelMA hydrogel scaffolds with different nHA contents, Journal of Bioactive and Compatible Polymers 37(5) (2022) 392-405.
[79] W. Jiao, X. Li, J. Shan, X. Wang, Study of several alginate-based hydrogels for in vitro 3D cell cultures, Gels 8(3) (2022) 147.
[80] P. Ma, W. Wu, Y. Wei, L. Ren, S. Lin, J. Wu, Biomimetic gelatin/chitosan/polyvinyl alcohol/nano-hydroxyapatite scaffolds for bone tissue engineering, Materials & Design 207 (2021) 109865.
[81] L. Guo, Z. Liang, L. Yang, W. Du, T. Yu, H. Tang, C. Li, H. Qiu, The role of natural polymers in bone tissue engineering, Journal of Controlled Release 338 (2021) 571-582.
[82] M.G. Kontakis, M. Moulin, B. Andersson, N. Norein, A. Samanta, C. Stelzl, A. Engberg, A. Diez-Escudero, J. Kreuger, N.P. Hailer, Trabecular-bone mimicking osteoconductive collagen scaffolds: an optimized 3D printing approach using freeform reversible embedding of suspended hydrogels, 3D Printing in Medicine 11(1) (2025) 11.
[83] I. Koumentakou, A. Michopoulou, M.J. Noordam, Z. Terzopoulou, D.N. Bikiaris, 3D-printed scaffolds for tissue engineering applications using thermosensitive hydrogels based on b iopolymer blends, Journal of Materials Science 59(20) (2024) 9021-9041.
[84] X. Yang, Y. Wang, Y. Zhou, J. Chen, Q. Wan, The application of polycaprolactone in three-dimensional printing scaffolds for bone tissue engineering, Polymers 13(16) (2021) 2754.
[85] M. Toledano, M. Toledano-Osorio, Á. Carrasco-Carmona, C. Vallecillo, C.D. Lynch, M.T. Osorio, R. Osorio, State of the art on biomaterials for soft tissue augmentation in the oral cavity. Part I: Natural polymers-based biomaterials, Polymers 12(8) (2020) 1850.
[86] A. Koyyada, P. Orsu, Recent advancements and associated challenges of scaffold fabrication techniques in tissue engineering applications, Regenerative Engineering and Translational Medicine 7 (2021) 147-159.
[87] W. Xu, S. Jambhulkar, D. Ravichandran, Y. Zhu, M. Kakarla, Q. Nian, B. Azeredo, X. Chen, K. Jin, B. Vernon, 3D printing-enabled nanoparticle alignment: a review of mechanisms and applications, Small 17(45) (2021) 2100817.
[88] Ö. ÇERLEK, M.A. KESERCİOĞLU, K. Han, Stereolithography (SLA): An Innovative Additive Manufacturing Process, New trends and frontiers in engineering (2024) 399-412.
[89] D. Chekkaramkodi, L. Jacob, R. Umer, H. Butt, Review of vat photopolymerization 3D printing of photonic devices, Additive Manufacturing 86 (2024) 104189.
[90] E. Hozdić, Characterization and comparative analysis of mechanical parameters of FDM-and SLA-Printed ABS materials, Applied Sciences 14(2) (2024) 649.
[91] M. Khorasani, E. MacDonald, D. Downing, A. Ghasemi, M. Leary, J. Dash, E.G. Sharabian, A. Almalki, M. Brandt, S. Bateman, Multi Jet Fusion (MJF) of polymeric components: A review of process, properties and opportunities, Additive Manufacturing (2024) 104331.
[92] S. Singh, D. Kaur, M. Singh, R. Balu, A. Mehta, H. Vasudev, Challenges and issues in manufacturing of components using polymer-based selective laser sintering (SLS): a review, International Journal on Interactive Design and Manufacturing (IJIDeM) (2024) 1-24.
[93] S.F. Darghiasi, A. Farazin, H.S. Ghazali, Design of bone scaffolds with calcium phosphate and its derivatives by 3D printing: A review, Journal of the Mechanical Behavior of Biomedical Materials 151 (2024) 106391.
[94] M.B. Kumar, P. Sathiya, M. Varatharajulu, Selective laser sintering, Advances in additive manufacturing processes, Bentham Science Publishers2021, pp. 28-47.
[95] F. Lupone, E. Padovano, F. Casamento, C. Badini, Process phenomena and material properties in selective laser sintering of polymers: A review, Materials 15(1) (2021) 183.
[96] L. Jauer, W. Meiners, S. Vervoort, C. Gayer, N.A. Zumdick, D. Zander, Selective laser melting of magnesium alloys, European Congress and Exhibition on Powder Metallurgy. European PM Conference Proceedings, The European Powder Metallurgy Association, 2016, pp. 1-6.
[97] I. Romanova-Bolshakova, A. Filimonov, N. Chernyshov, Automation of postprocessing parts and materials creating using the selective laser sintering technology, AIP Conference Proceedings, AIP Publishing, 2023.

[98] C. Yang, Z. Huan, X. Wang, C. Wu, J. Chang, 3D printed Fe scaffolds with HA nanocoating for bone regeneration, ACS Biomaterials Science & Engineering 4(2) (2018) 608-616.

[99] Y. Li, H. Jahr, K. Lietaert, P. Pavanram, A. Yilmaz, L. Fockaert, M. Leeflang, B. Pouran, Y. Gonzalez-Garcia, H. Weinans, Additively manufactured biodegradable porous iron, Acta biomaterialia 77 (2018) 380-393.

[100] P. Wen, Y. Qin, Y. Chen, M. Voshage, L. Jauer, R. Poprawe, J.H. Schleifenbaum, Laser additive manufacturing of Zn porous scaffolds: shielding gas flow, surface quality and densification, Journal of Materials Science & Technology 35(2) (2019) 368-376.

[101] M. Kumar, V. Sharma, Additive manufacturing techniques for the fabrication of tissue engineering scaffolds: a review, Rapid Prototyping Journal 27(6) (2021) 1230-1272.

[102] S. Diener, A. Zocca, J. Günster, Literature review: Methods for achieving high powder bed densities in ceramic powder bed based additive manufacturing, Open Ceramics 8 (2021) 100191.

[103] N. Betancourt, X. Chen, Review of extrusion-based multi-material bioprinting processes, Bioprinting 25 (2022) e00189.

[104] G. Bi, L. Mo, S. Liu, X. Zhong, J. Yang, Z. Yuan, S. Chen, L. Ren, DLP printed β-tricalcium phosphate functionalized ceramic scaffolds promoted angiogenesis and osteogenesis in long bone defects, Ceramics International 48(18) (2022) 26274-26286.

[105] H. Saijo, K. Igawa, Y. Kanno, Y. Mori, K. Kondo, K. Shimizu, S. Suzuki, D. Chikazu, M. Iino, M. Anzai, Maxillofacial reconstruction using custom-made artificial bones fabricated by inkjet printing technology, Journal of Artificial Organs 12(3) (2009) 200-205.

[106] P. Rider, Ž.P. Kačarević, S. Alkildani, S. Retnasingh, R. Schnettler, M. Barbeck, Additive manufacturing for guided bone regeneration: A perspective for alveolar ridge augmentation, International journal of molecular sciences 19(11) (2018) 3308.

[107] R. Pugliese, B. Beltrami, S. Regondi, C. Lunetta, Polymeric biomaterials for 3D printing in medicine: An overview, Annals of 3D Printed Medicine 2 (2021) 100011.

[108] N. Sultana, M.I. Hassan, M.M. Lim, Composite synthetic scaffolds for tissue engineering and regenerative medicine, Springer2015.

[109] F. Pati, J. Jang, J.W. Lee, D.-W. Cho, Extrusion bioprinting, Essentials of 3D biofabrication and translation, Elsevier2015, pp. 123-152.

[110] A. Mathew, S.R. Kishore, A.T. Tomy, M. Sugavaneswaran, S.G. Scholz, A. Elkaseer, V.H. Wilson, A. John Rajan, Vapour polishing of fused deposition modelling (FDM) parts: a critical review of different techniques, and subsequent surface finish and mechanical properties of the post-processed 3D-printed parts, Progress in Additive Manufacturing 8(6) (2023) 1161-11

[111] M. Mani, A. Karthikeyan, K. Kalaiselvan, P. Muthusamy, P. Muruganandhan, Optimization of FDM 3-D printer process parameters for surface roughness and mechanical properties using PLA material, Materials Today: Proceedings 66 (2022) 1926-1931.

[112] M. Heshmat, M. Adel, Investigating the effect of hot air polishing parameters on surface roughness of fused deposition modeling PLA products: ANOVA and regression analysis, Progress in Additive Manufacturing 6(4) (2021) 679-687.

[113] M. Heshmat, Y. Abdelrhman, Improving surface roughness of polylactic acid (PLA) products manufactured by 3D printing using a novel slurry impact technique, Rapid Prototyping Journal 27(10) (2021) 1791-1800.

[114] M. Heshmat, I. Maher, Y. Abdelrhman, Surface roughness prediction of polylactic acid (PLA) products manufactured by 3D printing and post processed using a slurry impact technique: ANFIS-based modeling, Progress in Additive Manufacturing 8(2) (2023) 87-98.

[115] M.S. Islam, A. Al-Fakhri, M.M. Rahman, Computer aided design/computer aided manufacturing (CAD/CAM) technology in the undergraduate dental programs in the MENA region, European Journal of Dental Education 28(1) (2024) 142-147.

[116] K. Fischer, M. Metz, M. Sekula, D. Katwal, D. Hannigan, T. Williams, Effect of educational intervention on computer-aided-design and computer-aided-manufacturing technology to preclinical dental students, European Journal of Dental Education 28(1) (2024) 320-327.

[117] T. Krastev, M. Payer, Z. Krastev, J.F.P. Cardelles, A. Vegh, D. Banyai, Z. Geczi, D. Vegh, The

utilisation of CAD/CAM technology amongst Austrian dentists: A pilot study, international dental journal 73(3) (2023) 430-434.

[118] M. Atef, A. Tarek, M. Shaheen, R.M. Alarawi, N. Askar, Horizontal ridge augmentation using native collagen membrane vs titanium mesh in atrophic maxillary ridges: Randomized clinical trial, Clinical implant dentistry and related research 22(2) (2020) 156-166.

[119] J. Sun, S. Yu, J. Wade-Zhu, Y. Wang, H. Qu, S. Zhao, R. Zhang, J. Yang, J. Binner, J. Bai, 3D printing of ceramic composite with biomimetic toughening design, Additive Manufacturing 58 (2022) 103027.

[120] N.W. Solís Pinargote, A. Smirnov, N. Peretyagin, A. Seleznev, P. Peretyagin, Direct ink writing technology (3d printing) of graphene-based ceramic nanocomposites: A review, Nanomaterials 10(7) (2020) 1300.

[121] C.-G. Liu, Y.-T. Zeng, R.K. Kankala, S.-S. Zhang, A.-Z. Chen, S.-B. Wang, Characterization and preliminary biological evaluation of 3D-printed porous scaffolds for engineering bone tissues, Materials 11(10) (2018) 1832.

[122] D. Behera, M. Cullinan, Current challenges and potential directions towards precision microscale additive manufacturing–Part I: Direct ink writing/jetting processes, Precision Engineering 68 (2021) 326-337.

[123] M. Zuo, N. Pan, Q. Liu, X. Ren, Y. Liu, T.-S. Huang, Three-dimensionally printed polylactic acid/cellulose acetate scaffolds with antimicrobial effect, RSC advances 10(5) (2020) 2952-2958.

[124] R. Liu, L. Ma, H. Liu, B. Xu, C. Feng, R. He, Effects of pore size on the mechanical and biological properties of stereolithographic 3D printed HAp bioceramic scaffold, Ceramics International 47(20) (2021) 28924-28931.

[125] Q. Chen, B. Zou, Q. Lai, K. Zhu, SLA-3d printing and compressive strength of PEGDA/nHAP biomaterials, Ceramics International 48(20) (2022) 30917-30926.

[126] G. Lee, M. Carrillo, J. McKittrick, D.G. Martin, E.A. Olevsky, Fabrication of ceramic bone scaffolds by solvent jetting 3D printing and sintering: Towards load-bearing applications, Additive Manufacturing 33 (2020) 101107.

[127] Y. Zeng, M. Zhou, S. Mou, J. Yang, Q. Yuan, L. Guo, A. Zhong, J. Wang, J. Sun, Z. Wang, Sustained delivery of alendronate by engineered collagen scaffold for the repair of osteoporotic bone defects and resistance to bone loss, Journal of Biomedical Materials Research Part A 10 8(12) (2020) 2460-2472.

[128] S. Aminnezhad, N.H. Hama, A.H. Hasan, F. Bagheri, M. Alavi, Applications of biocompatible polymeric nanomaterials in three-dimensional (3D) scaffolds: Bacterial infections and diabetes, International Journal of Biological Macromolecules (2025) 140331.

[129] B. Ameri, F. Taheri-Behrooz, Novel mixed mode I/II fracture load prediction of chitosan polymer-infiltrated hydroxyapatite ceramic scaffolds using ICIM/GMTS theory in bone scaffold additive manufacturing, Materials & Design 253 (2025) 113931.

[130] N. Suresh, A. Shanmugavadivu, N. Selvamurugan, Chitosan–exosome synergy: Advanced cell-free scaffold approaches for bone tissue engineering, International Journal of Biological Macromolecules (2025) 140753.

[131] D.O. Golubchikov, A.K. Petrov, V.A. Popkov, P.V. Evdokimov, V.I. Putlayev, Advances in the Fabrication of Polycaprolactone-Based Composite Scaffolds for Bone Tissue Engineering: From Chemical Composition to Scaffold Architecture, ACS Biomaterials Science & Engineering 11(6) (2025) 3201-3227.

[132] M. Batool, M.A. Abid, T. Javed, M.N. Haider, Applications of biodegradable polymers and ceramics for bone regeneration: a mini-review, International Journal of Polymeric Materials and Polymeric Biomaterials 74(1) (2025) 39-53.

[133] J. Sun, C. Chen, B. Zhang, C. Yao, Y. Zhang, Advances in 3D-printed scaffold technologies for bone defect repair: materials, biomechanics, and clinical prospects, BioMedical Engineering OnLine 24(1) (2025) 51.

[134] G. Mo, S. Wu, R. Guo, W. Qu, P. Shen, Camphene-based metallic ink for 3D-printed medical implants: Effect of hierarchical porous structure on mechanical and biological properties, Journal of Materials Science & Technology 248 (2026) 55-68.

[135] S.N. Kalva, I. Uysal, Z. Evis, A. Tezcaner, D. Keskin, A. Hegazy, T. Ibrahim, A.P. Kariyal, C.A.

Velasquez, M. Koç, Performance evaluation of 3D-printed PLA composites doped with WE43 magnesium alloy for bone tissue engineering applications, Biomaterials Advan ces (2025) 214414.

[136] K.-R. Zhang, H.-L. Gao, X.-F. Pan, P. Zhou, X. Xing, R. Xu, Z. Pan, S. Wang, Y. Zhu, B. Hu, Multifunctional bilayer nanocomposite guided bone regeneration membrane, Matter 1(3) (2019) 770-781.

[137] J.-G. Ji, J.-A. Yu, S.-H. Choi, D.-W. Lee, Clinical, radiographic, and histomorphometric evaluation of a vertical ridge augmentation procedure using a titanium-reinforced microporous expanded polytetrafluoroethylene membrane: a prospective case series with 1-year follow-up, Materials 14(14) (2021) 3828.

[138] K. Kim, Y. Su, A.J. Kucine, K. Cheng, D. Zhu, Guided bone regeneration using barrier membrane in dental applications, ACS Biomaterials Science & Engineering 9(10) (2023) 5457-5478.

[139] K. Kadam, V. Gadakh, Recent Advancement in Bioabsorbable Metals and Their Alloys for Implant Application—a Review, Journal of The Institution of Engineers (India): Series D (2024) 1-17.

[140] J.S. Lee, J.Y. Park, H.M. Chung, Y.W. Song, F.J. Strauss, Vertical ridge augmentation feasibility using unfixed collagen membranes and particulate bone substitutes: A 1-to 7-year retrospective single-cohort observational study, Clinical Implant Dentistry and Related Research 24(3) (2022) 372-381.

[141] F. Di Spirito, F. Giordano, M.P. Di Palo, C. Ferraro, L. Cecere, E. Frucci, M. Caggiano, R. Lo Giudice, Customized 3D-Printed Mesh, Membrane, Bone Substitute, and Dental Implant Applied to Guided Bone Regeneration in Oral Implantology: A Narrative Review, Dentistry Journal 12(10) (2024) 303.

[142] S.H. Han, M. Cha, Y.-Z. Jin, K.-M. Lee, J.H. Lee, BMP-2 and hMSC dual delivery onto 3D printed PLA-Biogel scaffold for critical-size bone defect regeneration in rabbit tibia, Biomedical Materials 16(1) (2020) 015019.

[143] J.-H. Shim, M.-C. Yoon, C.-M. Jeong, J. Jang, S.-I. Jeong, D.-W. Cho, J.-B. Huh, Efficacy of rhBMP-2 loaded PCL/PLGA/β-TCP guided bone regeneration membrane fabricated by 3D printing technology for reconstruction of calvaria defects in rabbit, Biomedical materials 9(6) (2014) 065006.

[144] J.-H. Shim, J.-Y. Won, S.-J. Sung, D.-H. Lim, W.-S. Yun, Y.-C. Jeon, J.-B. Huh, Comparative efficacies of a 3D-printed PCL/PLGA/β-TCP membrane and a titanium membrane for guided bone regeneration in beagle dogs, Polymers 7(10) (2015) 2061-2077.

[145] A. Alahnoori, M. Badrossamay, E. Foroozmehr, Characterization of hydroxyapatite powders and selective laser sintering of its composite with polyamide, Materials Chemistry and Physics 296 (2023) 127316.

[146] L. Lu, S.J. Peter, M.D. Lyman, H.-L. Lai, S.M. Leite, J.A. Tamada, S. Uyama, J.P. Vacanti, R. Langer, A.G. Mikos, In vitro and in vivo degradation of porous poly (DL-lactic-co-glycolic acid) foams, Biomaterials 21(18) (2000) 1837-1845.

[147] J.-H. Shim, J.-Y. Won, J.-H. Park, J.-H. Bae, G. Ahn, C.-H. Kim, D.-H. Lim, D.-W. Cho, W.-S. Yun, E.-B. Bae, Effects of 3D-printed polycaprolactone/β-tricalcium phosphate membranes on guided bone regeneration, International Journal of Molecular Sciences 18(5) (2017) 899.

[148] P. Windisch, K. Orban, G.E. Salvi, A. Sculean, B. Molnar, Vertical-guided bone regeneration with a titanium-reinforced d-PTFE membrane utilizing a novel split-thickness flap design: a prospective case series, Clinical oral investigations 25 (2021) 2969-2980.

[149] Q. Zhou, F. Yang, N. Li, Y.-F. Ren, Y. Yu, Healing outcomes of open versus closed flap procedures for collagen membrane coverage following immediate dental implant placements with simultaneous guided tissue regeneration, Journal of Dentistry 141 (2024

[150] W. Abd-Elaziem, M.A. Darwish, A. Hamada, W.M. Daoush, Titanium-Based alloys and composites for orthopedic implants Applications: A comprehensive review, Materials & Design (2024) 112850.

[151] K. Rahmouni, A. Besnard, K. Oulmi, C. Nouveau, A. Hidoussi, L. Aissani, M. Zaabat, In vitro corrosion response of CoCrMo and Ti-6Al-4V orthopedic implants with Zr columnar thin films, Surface and Coatings Technology 436 (2022) 128310.

[152] M. Hung, K. Sanders, A. Deshpande, R. Trivedi, C. Schwartz, A. Mohajeri, Guided Tissue Regeneration Membranes: Review of Innovations and Applications in Immunocompromised Patients, Applied Sciences 15(3) (2025) 1145.

[153] I. Antoniac, V. Manescu, A. Antoniac, G. Paltanea, Magnesium-based alloys with adapted interfaces

for bone implants and tissue engineering, Regenerative Biomaterials (2023) rbad095.

[154] P. Rider, Ž.P. Kačarević, A. Elad, D. Tadic, D. Rothamel, G. Sauer, F. Bornert, P. Windisch, D.B. Hangyási, B. Molnar, Biodegradable magnesium barrier membrane used for guided bone regeneration in dental surgery, Bioactive Materials 14 (2022) 152-168.

[155] M. Zhang, T. Gregory, U. Hansen, C.K. Cheng, Effect of stress-shielding-induced bone resorption on glenoid loosening in reverse total shoulder arthroplasty, Journal of Orthopaedic Research® 38(7) (2020) 1566-1574.

[156] Y. Shan, B. Qiao, S. Ouyang, C. Du, L. Zhao, G. Wang, J. Ye, Y. Xiong, Y. Wei, J. Song, Biodegradable Mg-Ca/Mg-Cu bilayer membranes with enhanced mechanical, osteogenesis and antibacterial performances for GBR applications, Journal of Magnesium and Alloys 13(2) (2025) 792-809.

[157] J. Wu, X. Cheng, J. Wu, J. Chen, X. Pei, The development of magnesium-based biomaterials in bone tissue engineering: a review, Journal of Biomedical Materials Research Part B: Applied Biomaterials 112(1) (2024) e35326.

[158] F. Soares, C.N. Elias, E.S. Monteiro, M.E.R. Coimbra, A.I.C. Santana, Galvanic corrosion of Ti dental implants coupled to CoCrMo prosthetic component, International Journal of Biomaterials 2021 (2021).

[159] Z.-Y. Yan, J.-H. Zhu, G.-Q. Liu, Z.-C. Liu, C.-B. Guo, N.-H. Cui, J.-M. Han, Feasibility and Efficacy of a Degradable Magnesium-Alloy GBR Membrane for Bone Augmentation in a Distal Bone-Defect Model in Beagle Dogs, Bioinorganic Chemistry and Applications 2022 (2022).

[160] S. Wu, Y.-S. Jang, Y.-K. Kim, S.-Y. Kim, S.-O. Ko, M.-H. Lee, Surface Modification of pure magnesium mesh for guided bone regeneration: in vivo evaluation of rat calvarial defect, Materials 12(17) (2019) 2684.

[161] H. Saito, E. Couso-Queiruga, H.J. Shiau, S. Stuhr, H. Prasad, T.V. Allareddy, M.A. Reynolds, G. Avila-Ortiz, Evaluation of poly lactic-co-glycolic acid-coated β-tricalcium phosphate for alveolar ridge preservation: A multicenter randomized controlled trial, Journal of Periodontology 92(4) (2021) 524-535.

[162] X. Yang, Y. Ma, X. Wang, S. Yuan, F. Huo, G. Yi, J. Zhang, B. Yang, W. Tian, A 3D-bioprinted functional module based on decellularized extracellular matrix bioink for periodontal regeneration, A dvanced Science 10(5) (2023) 2205041.

[163] S.E. Alavi, M. Gholami, H.E. Shahmabadi, P. Reher, Resorbable GBR scaffolds in oral and maxillofacial tissue engineering: design, fabrication, and applications, Journal of Clinical Medicine 12(22) (2023) 6962.

[164] C. Liu, Z. Peng, H. Xu, H. Gao, J. Li, Y. Jin, Y. Wang, C. Wang, Y. Liu, Y. Hu, 3D printed platelet-rich plasma-loaded scaffold with sustained cytokine release for bone defect repair, Tissue Engineering Part A 28(15-16) (2022) 700-711.

[165] P. Kumar, Shamim, M. Muztaba, T. Ali, J. Bala, H.S. Sidhu, A. Bhatia, Fused deposition modeling 3D-printed scaffolds for bone tissue engineering applications: a review, Annals of Biomedical Engineering 52(5) (2024) 1184-1194.

[166] A.S. Alagoz, V. Hasirci, 3D printing of polymeric tissue engineering scaffolds using open-source fused deposition modeling, Emergent Materials 3(4) (2020) 429-439.

[167] K. Glover, E. Mathew, G. Pitzanti, E. Magee, D.A. Lamprou, 3D bioprinted scaffolds for diabetic wound-healing applications, Drug delivery and translational research 13(8) (2023) 2096-2109.

[168] A. Khojasteh, H. Behnia, F.S. Hosseini, M.M. Dehghan, P. Abbasnia, F.M. Abbas, The effect of PCL-TCP scaffold loaded with mesenchymal stem cells on vertical bone augmentation in dog mandible: a preliminary report, Journal of Biomedical Materials Research Part B: Applied Biomaterials 101(5) (2013) 848-854.

[169] P.S. Kumar, S. Hashimi, S. Saifzadeh, S. Ivanovski, C. Vaquette, Additively manufactured biphasic construct loaded with BMP-2 for vertical bone regeneration: A pilot study in rabbit, Materials Science and Engineering: C 92 (2018) 554-564.

[170] C.X. Lam, S.H. Teoh, D.W. Hutmacher, Comparison of the degradation of polycaprolactone and polycaprolactone–(β-tricalcium phosphate) scaffolds in alkaline medium, Polymer international 56(6) (2007) 718-728.

[171] M. Bartnikowski, T.R. Dargaville, S. Ivanovski, D.W. Hutmacher, Degradation mechanisms of

polycaprolactone in the context of chemistry, geometry and environment, Progress in Polymer Science 96 (2019) 1-20.

[172] B.T. Goh, N. Chanchareonsook, H. Tideman, S.H. Teoh, J.K.F. Chow, J.A. Jansen, The use of a polycaprolactone–tricalcium phosphate scaffold for bone regeneration of tooth socket facial wall defects and simultaneous immediate dental implant placement in Macaca fascicularis, Journal of Biomedical Materials Research Part A 102(5) ( 2014) 1379-1388.

[173] A. Frag, A. Abdal-hay, P. Han, S. Ivanovski, Fabrication of 3D melt electrowritting Multiphasic scaffold with bioactive and osteoconductivite functionalities for periodontal regeneration, Ceramics International (2022).

[174] G.M.H. Ortiz, R. Parra, J. Fraile-Sainz, C. Domingo, M.A. Fanovich, Porous hydroxyapatite-titanium dioxide composites prepared by a sol-gel/supercritical CO2-drying combined process, Ceramics International 50(8) (2024) 13298-13307.

[175] M. Mobaraki, M. Ghaffari, A. Yazdanpanah, Y. Luo, D. Mills, Bioinks and bioprinting: A focused review, Bioprinting 18 (2020) e00080.

[176] M. Salehi, S. Maleksaeedi, M.A.B. Sapari, M.L.S. Nai, G.K. Meenashisundaram, M. Gupta, Additive manufacturing of magnesium–zinc–zirconium (ZK) alloys via capillary-mediated binderless three-dimensional printing, Materials & Design 169 (2019) 107683.

[177] X. Zhang, X.-W. Li, J.-G. Li, X.-D. Sun, Preparation and mechanical property of a novel 3D porous magnesium scaffold for bone tissue engineering, Materials Science and Engineering: C 42 (2014) 362-367.

[178] T. Lin, X. Wang, L. Jin, W. Li, Y. Zhang, A. Wang, J. Peng, H. Shao, Manufacturing of porous magnesium scaffolds for bone tissue engineering by 3D gel-printing, Materials & Design 209 (2021) 109948.

[179] D. Huang, Z. Li, G. Li, F. Zhou, G. Wang, X. Ren, J. Su, Biomimetic structural design in 3D-printed scaffolds for bone tissue engineering, Materials Today Bio (2025) 101664.

[180] S. Wang, R. Gu, F. Wang, X. Zhao, F. Yang, Y. Xu, F. Yan, Y. Zhu, D. Xia, Y. Liu, 3D-Printed PCL/Zn scaffolds for bone regeneration with a dose-dependent effect on osteogenesis and osteoclastogenesis, Materials Today Bio 13 (2022) 100202.

[181] G. García-García, M. Lázaro-Callejón, F. Fernández-Álvarez, G.R. Iglesias, J.L. Arias, (Magnetite/poly (ε-caprolactone))/chitosan (core/shell)/shell nanocomposites with potential applications in hyperthermia cancer therapy, Journal of Magnetism and Magnetic Materials (2023) 171500.

[182] S. Zhao, K. Xie, Y. Guo, J. Tan, J. Wu, Y. Yang, P. Fu, L. Wang, W. Jiang, Y. Hao, Fabrication and biological activity of 3D-printed polycaprolactone/magnesium porous scaffolds for critical size bone defect repair, ACS Biomaterials Science & Engineering 6(9) (2020) 5120-5131.

[183] R.B. Indaryanti, H. Harsono, S. Sutama, B. Murtiyasa, B. Soemardjoko, 4D research and development model: Trends, challenges, and opportunities review, Jurnal Kajian Ilmiah 25(1) (2025) 91-98.

[184] C. Shen, A. Shen, 4D printing: innovative solutions and technological advances in orthopedic repair and reconstruction, personalized treatment and drug delivery, BioMedical Engineering OnLine 24(1) (2025) 5.

[185] M. Günay, T. Meral, Biomedical Applications with Multiscale Structures Produced by Additive Manufacturing, Journal of Molecular and Engineering Materials 13(01) (2025) 2430004.

[186] A. Bandyopadhyay, A. Dash, S. Bose, Additive Manufacturing of Multi-Material Structures, Additive Manufacturing, CRC Press, pp. 244-266.

[187] T. Kawai, Preclinical Evaluation and Advancements in Vascularized Bone Tissue Engineering, Biomimetics 10(7) (2025) 412.